Ecological Monographs, 79(1), 2009, pp. 25–58

Predicting 21st-century polar bear habitat distribution from global climate models

GEORGE M. DURNER,[1,15] DAVID C. DOUGLAS,[2] RYAN M. NIELSON,[3] STEVEN C. AMSTRUP,[1] TRENT L. MCDONALD,[3] IAN STIRLING,[4] METTE MAURITZEN,[5] ERIK W. BORN,[6] ØYSTEIN WIIG,[7] ERIC DEWEAVER,[8] MARK C. SERREZE,[9] STANISLAV E. BELIKOV,[10] MARIKA M. HOLLAND,[11] JAMES MASLANIK,[12] JON AARS,[13] DAVID A. BAILEY,[11] AND ANDREW E. DEROCHER[14]

[1]*U.S. Geological Survey, Alaska Science Center, 4210 University Drive, Anchorage, Alaska 99508 USA*
[2]*U.S. Geological Survey, Alaska Science Center, 3100 National Park Road, Juneau, Alaska 99801 USA*
[3]*Western EcoSystems Technology, Inc., 2003 Central Avenue, Cheyenne, Wyoming 82001 USA*
[4]*Canadian Wildlife Service, 5320-122 Street, Edmonton, Alberta T6H 3S5 Canada*
[5]*Marine Mammal Research Group, Institute of Marine Research, Poboxs 1870 Nordnes, 5817 Bergen, Norway*
[6]*Greenland Institute of Natural Resources, P.O. Box 570, DK-3900, Nuuk, Greenland*
[7]*Natural History Museum, University of Oslo, P.O. Box 1172, Blindern N-0318, Oslo, Norway*
[8]*Center for Climate Research, Atmospheric and Oceanic Sciences Department,*
University of Wisconsin, Madison, Wisconsin 53706 USA
[9]*Cooperative Institute for Research in Environmental Sciences, National Snow and Ice Data Center, Campus Box 449,*
University of Colorado, Boulder, Colorado 80309 USA
[10]*All-Russian Research Institute for Nature Protection, Znamenskoye-Sadki, Moscow, Russian Federation*
[11]*National Center for Atmospheric Research, 1850 Table Mesa Drive, Boulder, Colorado 80305 USA*
[12]*Department of Aerospace Engineering Sciences, CCAR, Campus Box 431, University of Colorado, Boulder, Colorado 80309 USA*
[13]*Norwegian Polar Institute, Polarmiljøsenteret, N-9296, Tromsø, Norway*
[14]*Department of Biological Sciences, University of Alberta, Edmonton, Alberta T6G 2E9 Canada*

Abstract. Projections of polar bear (*Ursus maritimus*) sea ice habitat distribution in the polar basin during the 21st century were developed to understand the consequences of anticipated sea ice reductions on polar bear populations. We used location data from satellite-collared polar bears and environmental data (e.g., bathymetry, distance to coastlines, and sea ice) collected from 1985 to 1995 to build resource selection functions (RSFs). RSFs described habitats that polar bears preferred in summer, autumn, winter, and spring. When applied to independent data from 1996 to 2006, the RSFs consistently identified habitats most frequently used by polar bears. We applied the RSFs to monthly maps of 21st-century sea ice concentration projected by 10 general circulation models (GCMs) used in the Intergovernmental Panel of Climate Change Fourth Assessment Report, under the A1B greenhouse gas forcing scenario. Despite variation in their projections, all GCMs indicated habitat losses in the polar basin during the 21st century. Losses in the highest-valued RSF habitat (optimal habitat) were greatest in the southern seas of the polar basin, especially the Chukchi and Barents seas, and least along the Arctic Ocean shores of Banks Island to northern Greenland. Mean loss of optimal polar bear habitat was greatest during summer; from an observed 1.0 million km^2 in 1985–1995 (baseline) to a projected multi-model mean of 0.32 million km^2 in 2090–2099 (−68% change). Projected winter losses of polar bear habitat were less: from 1.7 million km^2 in 1985–1995 to 1.4 million km^2 in 2090–2099 (−17% change). Habitat losses based on GCM multi-model means may be conservative; simulated rates of habitat loss during 1985–2006 from many GCMs were less than the actual observed rates of loss. Although a reduction in the total amount of optimal habitat will likely reduce polar bear populations, exact relationships between habitat losses and population demographics remain unknown. Density and energetic effects may become important as polar bears make long-distance annual migrations from traditional winter ranges to remnant high-latitude summer sea ice. These impacts will likely affect specific sex and age groups differently and may ultimately preclude bears from seasonally returning to their traditional ranges.

Key words: climate change; general circulation model; IPCC; passive microwave; polar basin; polar bear; radio telemetry; resource selection function; sea ice; SMMR; SSM/I; Ursus maritimus.

Manuscript received 19 December 2007; revised 31 March 2008; accepted 4 April 2008. Corresponding Editor: M. Wikelski.

[15] E-mail: gdurner@usgs.gov

INTRODUCTION

Contemporary observations and state of the art models indicate a warming global climate, with some of the most accelerated changes taking place in Arctic and subarctic habitats. Habitat loss has been implicated as the greatest threat to the survival of most species (Wilcove et al. 1998, Groom and Vynne 2006). Furthermore, extinction theory suggests that the most vulnerable species are those that are specialized (Davies et al. 2004), long lived with long generation times and low reproductive output (Bodmer et al. 1997), and are carnivores with a large geographic extent and low population densities (Viranta 2003). The habitats and life history characteristics of polar bears (*Ursus maritimus*; Amstrup 2003) fit the description of a species vulnerable to environmental change, specifically, loss of the Arctic sea ice cover as the climate warms. Here we attempt to understand how projected warming of the polar region may affect polar bears by looking at changes in projected quantity and quality of sea ice habitat. Knowledge of how habitats are likely to change in the near future is crucial for understanding how changes in habitat could affect population dynamics and for developing an appropriate adaptive management response.

The distribution and composition of Arctic sea ice is pivotal for the survival of wild populations of polar bears (Amstrup 2003). Polar bears evolved during the middle Pleistocene (Kurten 1964) as highly specialized surface-based predators on sea ice dependent phocid seals, primarily ringed seals (*Phoca hispida*) and bearded seals (*Erignathus barbatus*; Stirling and Archibald 1977). The sea ice allows polar bears to exploit the productive marine environment by providing a platform from which they can hunt seals. Polar bears also evolved in an environment that has been largely free of competitors and predators, with the exception of humans in nearshore areas and other polar bears. This isolation has allowed polar bears to flourish on the floating sea ice cover.

There are currently estimated to be ~24 600 polar bears (Aars et al. 2006) distributed over a maximum of 1.5×10^7 km^2 of northern hemisphere sea ice (mean 1979–2006 winter estimate; National Snow and Ice Data Center, Boulder, Colorado, USA; Cavalieri et al. 2006, Meier et al. 2006). Polar bears are not distributed uniformly on Arctic sea ice but instead appear to select specific sea ice features (Stirling et al. 1993, Arthur et al. 1996, Ferguson et al. 2000, 2001, Mauritzen et al. 2001, Durner et al. 2004, 2006). Sea ice over and near the continental shelf appears to be preferred habitat (Derocher et al. 2004, Durner et al. 2004), likely because of higher biological productivity there, relative to deep-water regions of the central polar basin (Pomeroy 1997, Sakshaug 2003, Dunton et al. 2005), and greater biomass and accessibility of prey in nearshore shear zones and polynyas (areas of open water surrounded by sea ice; Stirling 1997). Furthermore, the stable land-fast ice over the continental shelf, where snow drifts develop that are suitable for the excavation of ringed-seal birth lairs, provides habitat where ringed seals are both abundant and accessible (Smith and Stirling 1975, Stirling et al. 1993). However, in addition to selecting habitats based on prey availability, polar bears may also select areas of relatively high sea ice concentration because these habitats are more stable and thus safer during storms (Mauritzen et al. 2003*a*).

Nineteen polar bear subpopulations are currently recognized by the International Union for the Conservation of Nature and Natural Resources (IUCN) Polar Bear Specialist Group (PBSG; Aars et al. 2006). Based on movements of radio-collared female polar bears, there are varying degrees of overlap among subpopulations (Bethke et al. 1996, Taylor et al. 2001, Mauritzen et al. 2002, Amstrup et al. 2004). Despite this observed overlap, however, the discrete boundaries used by the IUCN are effective for addressing management concerns throughout the range of polar bears (Aars et al. 2006) and are remarkably concordant with regional sea ice characteristics (Meier et al. 2007, Overland and Wang 2007). Throughout this paper, we use the term "subpopulation" in a manner consistent with that of Aars et al. (2006).

In the past 30 years, mean world surface temperatures have increased 0.2°C per decade, but in some parts of the Arctic, temperatures have increased at 10 times this rate (Hansen et al. 2006). Since the late 1970s (the advent of routine monitoring via satellite remote sensing), there have been major reductions in summer sea ice extent (Meier et al. 2007), decreases in the extent and age of multiyear ice (Rigor and Wallace 2004, Belchansky et al. 2005, Maslanik et al. 2007*b*) and thickness (Rothrock et al. 1999, Tucker et al. 2001), and increases in length of the summer melt period (Belchansky et al. 2004, Stroeve et al. 2005). Though satellite data from 1979 to 2006 show that September sea ice extent has declined at a rate of 8.6% per decade, September 2007 set a new record minimum that was 23% lower than the previous 2005 record (NSIDC, data *available online*).[16] Winter sea ice has also started to decline, but at a slower rate than in summer (Comiso 2006, Serreze et al. 2007). Hence, empirical evidence confirms the environment on which polar bears depend for their survival has already changed substantially.

Future climate simulations from coupled ocean–atmosphere general circulation models (GCMs) show continued reductions in ice extent and multiyear ice throughout the 21st century (Holland et al. 2006, Zhang and Walsh 2006, Overland and Wang 2007) in probable response to increases in greenhouse gas concentrations (Serreze et al. 2007, Stroeve et al. 2007). The projections of 21st-century sea ice declines, however, appear to be conservative because the observed rate of sea ice loss over the period of available observations is greater than that estimated by most GCMs from the Intergovern-

---

[16] ⟨http://nsidc.com⟩

mental Panel on Climate Change (IPCC) Fourth Assessment Report (AR-4) (Stroeve et al. 2007).

Without sea ice, polar bears lose the platform they are dependent upon for almost all of their seal hunting opportunities. An earlier spring break up and increases in the duration of the summer melt season, when polar bears are restricted to land or forced over relatively unproductive Arctic waters, may compromise their hunting success, thereby reducing individual survival or reproductive success and ultimately reducing population size (Derocher et al. 2004, Stirling and Parkinson 2006). Apart from hauling out on the ice for the annual molt, phocid seals do not need sea ice during summer and so are largely inaccessible to polar bears during extensive summer melting (Harwood and Stirling 1992). Unusual movements, such as long distance swims to reach pack (drift) ice or land make polar bears vulnerable to mortality in stormy weather (Monnett and Gleason 2006).

A continued decline in the total amount of optimal sea ice habitat for hunting seals may impose nutritional stress on polar bears and cause them to resort to novel food sources including cannibalism (Amstrup et al. 2006) and anthropogenic foods (Stirling and Parkinson 2006). It is, however, unlikely that terrestrial foods can be a significant source of nutrition for land-bound polar bears (Ramsay and Hobson 1991). In an environment where the duration of the open water period is increasing, polar bears must often endure longer periods with little or no hunting opportunities, and often with less stored fat to survive upon. Such effects have been definitively linked to a decline in at least one population: Western Hudson Bay, located at the southern end of the species' range (Stirling and Parkinson 2006, Regehr et al. 2007).

In 2005, the IUCN Polar Bear Specialist Group (PBSG) unanimously agreed that the world population of polar bears may decrease by more than 30% during the next ~45 years (i.e., three polar bear generations) due to projected decreases in sea ice (Aars et al. 2006). In January 2007, the U.S. Fish and Wildlife Service (USFWS) proposed listing the polar bear as a threatened species under the Endangered Species Act (USFWS 2007). To help inform their final decision, we conducted this analysis of polar bear sea ice habitats using empirical data to quantify relationships between polar bear distributions and sea ice conditions (and other constant environmental factors such as bathymetry and distance to shore) by constructing resource selection functions (RSF). We then extrapolated the RSF models using projections of future sea ice distribution to estimate trends in the amount, quality, and location of polar bear sea ice habitat into the 21st century.

METHODS

Study area

Characteristic patterns of ice drift in the polar basin (Rigor et al. 2002) and the paleoclimate records (Kaufman et al. 2004, CAPE Last Interglacial Project Members 2006) prompted Amstrup et al. (2007) to define a Divergent ecoregion that included peripheral regions of the polar basin (subpopulations: Barents Sea, Chukchi Sea, Kara Sea, Laptev Sea, and Southern Beaufort Sea; Fig. 1) where annual ice is formed but is either exported to other regions or melts and retreats toward the central basin during the following summer. Polar bears in the Divergent ecoregion have the opportunity to follow the sea ice as it retreats into the polar basin during summer or they may abandon the ice to summer on land.

Within the polar basin, Amstrup et al. (2007) also defined a region of convergent sea ice ("Convergent" ecoregion). In the Convergent ecoregion, sea ice is present in the central Arctic throughout the year and much of this sea ice originates in the Divergent ecoregion. The Beaufort Gyre and the Transpolar Drift Stream result in accumulation of persistent and older sea ice on the northern shores of Canadian Archipelago islands, northern Greenland, and in the East Greenland Sea (Rigor et al. 2002, Rigor and Wallace 2004). These ice dynamics allow polar bears in the Convergent ecoregion to occupy nearshore sea ice throughout the year. Subpopulations in the Convergent ecoregion include the Arctic Basin, East Greenland Sea, and Northern Beaufort Sea (Fig. 1). Following Amstrup et al. (2007), we recognized an additional Convergent ecoregion "subpopulation," named Queen Elizabeth (Fig. 1) because it includes a recurring nearshore lead system (Stirling 1980) and an estimated population of 200 polar bears (Lunn et al. 1995).

Amstrup et al. (2007) described a Seasonal Ice and an Archipelago ecoregion (Fig. 1). Both the Seasonal Ice and Archipelago ecoregions include an estimated 7700 and 5000 polar bears, respectively (Aars et al. 2006). We excluded the Seasonal Ice and Archipelago ecoregions from this report, however, because polar bear tracking data in those locations were largely unavailable for our analysis. The Divergent and Convergent ecoregions collectively include ~11 900 of the world's estimated 24 600 polar bears (Aars et al. 2006). Abundant polar bear location data were available for these two regions (see *Methods: Polar bear location data*), therefore we focused our analyses on polar bear habitat relationships within the Divergent and Convergent ecoregions.

Because our focus was on projecting future sea ice habitat, our study considers only the composition and distribution of sea ice habitats and does not consider open ocean or land habitats. We excluded open ocean because it is rarely used by polar bears (Arthur et al. 1996, Mauritzen et al. 2003*a*, Durner et al. 2006) except when attempting to reach pack ice or land (Monnett and Gleason 2006). In the polar basin, polar bears have been observed to abandon sea ice for land during summer (Mauritzen et al. 2001, Kochnev 2006; USFWS, *unpublished data*), but with the exception of Svalbard (Mauritzen et al. 2001), the number of polar bears that

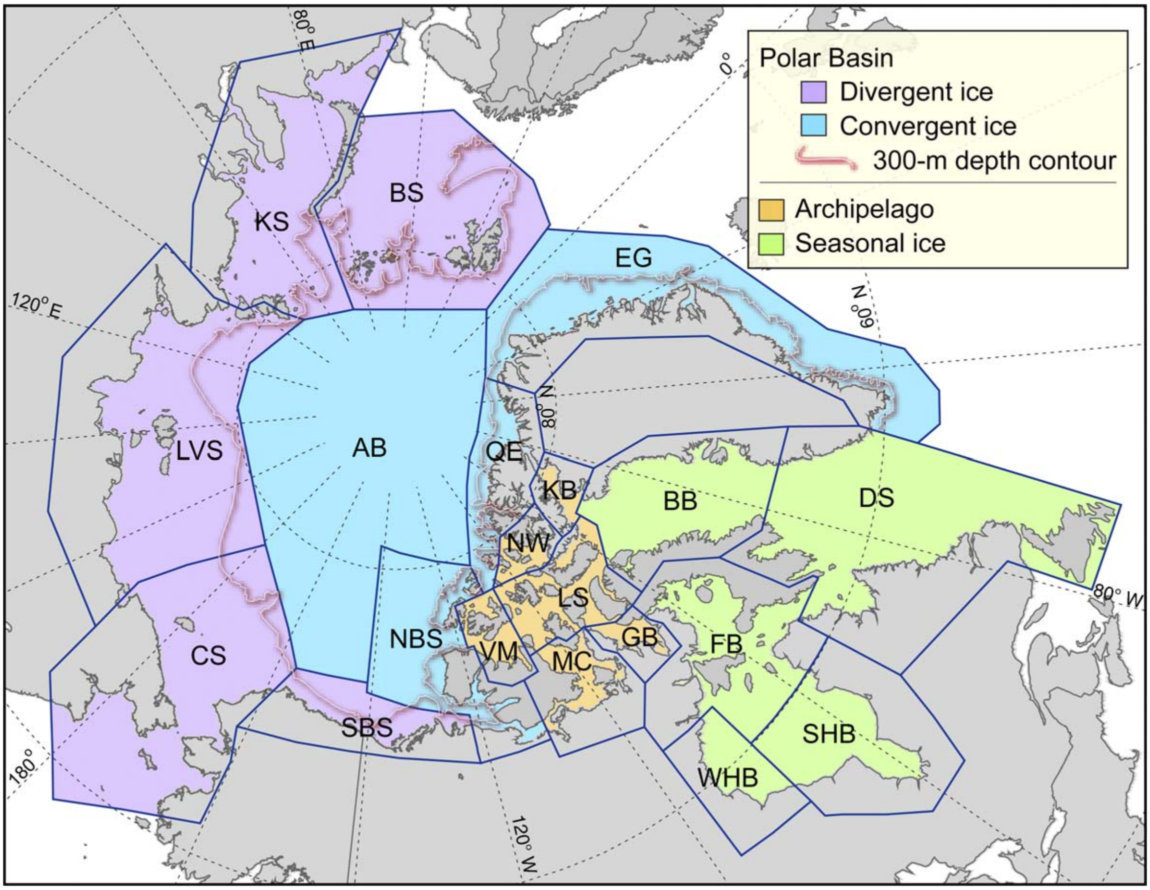

Fig. 1. The polar basin RSF study area, defined by a composite of IUCN polar bear subpopulation units located in the Arctic Ocean and peripheral seas (pelagic region). Units are color-shaded to distinguish membership within two groups based on general sea ice dynamics: "Divergent" (purple) where ice is generally advected offshore (and melts away from shore during summer) and "Convergent" (blue) where ice motion promotes convergence and shoreward drift year round. Polar bears inhabit two other ecoregions (Archipelago and Seasonal) in northeast North America, but these regions were not part of our study area due to insufficient samples of polar bear tracking data and dramatically different sea ice characteristics. Key to abbreviations: Barents Sea (BS), Kara Sea (KS), Laptev Sea (LVS), Chukchi Sea (CS), Southern Beaufort Sea (SBS), Northern Beaufort Sea (NBS), Arctic Basin (AB), Queen Elizabeth (QE), and East Greenland (EG), Kane Basin (KB), Norwegian Bay (NW), Viscount Melville Sound (VM), Lancaster Sound (LS), M'Clintock Channel (MC), and Gulf of Boothia (GB), Baffin Bay (BB), Davis Strait (DS), Foxe Basin (FB), Western Hudson Bay (WHB), and Southern Hudson Bay (SHB).

summer on land in the polar basin is small relative to the size of their respective subpopulation (Kochnev 2006; USFWS, *unpublished data*). Furthermore, polar bears on land generally feed very little, they attempt to conserve energy, and they immediately return to sea once ice forms in autumn (Derocher and Stirling 1990, Ramsay and Hobson 1991). Consequently, land habitats generally contribute a small amount to the annual energy budget of polar bears.

Polar bear location data

We used location data from satellite radio collars deployed on adult female polar bears representing several subpopulations over the period of 1985–2006. The majority of data came from polar bears marked in the Bering, eastern Chukchi, and Beaufort seas by the USGS. Data from bears in the western Chukchi, Kara, and Laptev seas were from joint research by the USGS and the All-Russian Research Institute for Nature Protection. Data were also obtained from polar bears marked in Canadian regions of the Beaufort Sea (1992–1995) by the Canadian Wildlife Service, and from Viscount Melville Sound (1989–1993) by the University of Saskatchewan. Polar bear location data from the Barents Sea (1988–1999) were provided by the Norwegian Polar Institute and the All-Russian Research Institute for Nature Protection, and data from the East Greenland Sea (1993–1994) were provided by the Greenland Institute of Natural Resources. Polar bears were captured with standard animal immobilization techniques (Stirling et al. 1989) during March–June and August–November.

The majority of bears were equipped with satellite radio collars (platform transmitter terminal, or PTT; Telonics, Mesa, Arizona, USA) that transmitted signals from which locations were calculated by the Argos Data Collection and Location System (ADCLS; Fancy et al. 1988). Most PTTs transmitted for 4–8 hours every 1–7 days (duty cycle). Several locations were typically obtained during each duty cycle. For analysis we used standard-quality locations only (Argos location classes 1, 2, or 3), which are generally accurate to within 1.2 km (Keating et al. 1991).

In 2004–2006, the majority of satellite radio collars deployed by the USGS in the Beaufort Sea used Global Positioning System (GPS; Telonics, Mesa, Arizona, USA) technology for location determination. Locations calculated by a GPS receiver within the collar were then transmitted to the USGS via ADCLS. Both PTTs and GPS satellite-radio collars typically collected several high-quality locations per duty cycle.

For both ADCLS and GPS locations, we randomly selected one location per bear per day. From these, we retained only those locations that were within our study area. Most pregnant polar bears occupy maternal dens between October and April (Amstrup and Gardner 1994). To eliminate the potential bias resulting from denning polar bears, we used observational (Amstrup and Gardner 1994) and temperature- and activity-sensor data (Fischbach et al. 2007) to identify and remove all locations during the time that they were known to be in dens.

For analysis, we divided the polar bear location data into two decadal time periods based on differences in collaring effort and sea ice conditions: 1985–1995 and 1996–2006. We based this separation on three considerations. First, the reduced sampling effort during 1995–1996 (Table 1) provided a convenient break at a midpoint during the two decades of radio-tracking data. Second, given the more extensive sea ice of the earlier decade (Ogi and Wallace 2007), polar bear movements were less restricted compared to 1996–2006. Third, the 1985–1995 tracking data better represented all polar bear subpopulations throughout the Arctic basin (Table 1). After 1995, however, the proportion of polar bear location data in the Chukchi, Laptev, and Kara seas was greatly reduced, while the proportion from the Southern Beaufort Sea essentially doubled (60.7% after 1995 vs. 30.9% prior to 1996). We therefore postulated that RSF models derived from 1985 to 1995 data would more accurately represent resource selection across the study area under historical ice regimes than would models developed from more recent data; hence, the 1985–1995 period was used as the baseline period to determine polar bear habitat selection indices. Finally, building the RSF models from the 1985–1995 data also allowed us to examine the degree of change in polar bear habitats between the two time periods, using strictly observational data.

Observational habitat data

Estimates of monthly sea ice concentration (Cavalieri et al. 2006) derived from satellite passive microwave (PMW) brightness temperatures were obtained from the National Snow and Ice Data Center. The PMW sea ice concentration data were disseminated in raster format with a 25 × 25 km pixel size in polar stereographic projection. The polar-orbiting PMW sensors do not view a small region around the North Pole due to an inclination in the satellite orbits. We set missing data within this "pole hole" to 100% ice concentration, since based on field observations and other satellite data, this high-latitude region is known to have been almost completely ice covered during the entire study period.

Estimates of ocean depth were based on the International Bathymetric Chart of the Arctic Ocean (IBCAO; Jakobsson et al. 2000). The IBCAO data were distributed in a polar stereographic projection grid with 2.5-km pixel resolution. We resampled the native bathymetry grid to 25-km pixel resolution (identical to PMW) by averaging depth within the boundaries of each PMW pixel.

General circulation model data

We extrapolated the RSF models (described later) using monthly sea ice concentration grids from 10 GCM outputs produced for the Intergovernmental Panel of Climate Change (IPCC) Fourth Assessment Report (AR-4; IPCC 2007; Table 2). We used sea ice projections for the 21st century from model runs that were forced with a middle-range greenhouse gas emission scenario, the A1B scenario ($CO_2 \approx 720$ ppm by 2100) of the Special Report on Emission Scenarios (Nakicencovic and Swart 2000). For the Community Climate System Model version 3 (CCSM3), we also extrapolated the RSFs using 21st-century ice projections based on the more conservative SRES-B1 scenario, which reflects a more gradual increase in greenhouse gas concentration ($CO_2 \approx 550$ ppm by 2100). We also used hindcast sea ice concentration outputs from model runs that simulated the 20th-century climate based on observed natural and anthropogenic environmental forcing (20C3M; Meehl et al. 2005). We obtained all GCM data from the World Climate Research Programme's (WCRP) Coupled Model Intercomparison Project Phase 3 (CMIP3) multi-model data set (data *available online*),[17] except CCSM3 which we obtained directly from the National Center for Atmospheric Research (NCAR) in its native CCSM grid format. We obtained and analyzed one ensemble member (run-1) for each GCM, except CCSM3, for which we obtained eight runs.

We selected the 10 GCMs (Table 2) from a larger group of 20 based on an analysis of concordance (DeWeaver 2007) between their 20th-century simulations (20C3M) of September sea ice extent and the observational record of September ice extent, averaged over the period 1953–1995. Overland and Wang (2007) summarized performance of all AR-4 GCMs in their ability to simulate observed sea ice extent in various

[17] ⟨https://esg.llnl.gov:8443⟩

Table 1. Numbers of polar bear locations in pelagic Conservation of Nature and Natural Resources (IUCN) subpopulations by year used for estimating (1985–1995) and evaluating (1996–2006) Resource Selection Functions (RSF).

	RSF derivation period (1985–1995)											
	Year											
IUCN Unit	1985	1986	1987	1988	1989	1990	1991	1992	1993	1994	1995	Total
Chukchi Sea	3	184	301	375	343	892	603	648	694	270		4313
S. Beaufort Sea	87	302	326	495	677	283	332	709	403	148		3762
Laptev Sea		3		23	404	415	167	249	322	52	7	1642
Arctic Basin	8	96	143	67	302	228	36	116	221	148	7	1372
Barents Sea					15	6	89	103	101	95	109	518
N. Beaufort Sea				11	2	16	6	37	109	116		297
E. Greenland								3	35	38	62	138
Kara Sea							31	37		61		129
Total	98	585	770	971	1743	1840	1264	1902	1885	928	185	12 171

Note: Empty cells indicate that no data are available.

regions in the Arctic, and they concluded by recommending that some form of model selection criteria is warranted when using the AR-4 GCMs to project future sea ice conditions. Specifically, the GCMs we selected simulated mean northern hemisphere September ice extent during 1953–1995 to within 20% of the observed mean in the Hadley Center sea ice and surface temperature data set (HadISST; Rayner et al. 2003). Our selection method emulated the procedure used by Stroeve et al. (2007), except that we used a 50% ice concentration threshold to define ice extent (as opposed to 15%). We chose a 50% threshold because other studies have shown that polar bears select medium to high sea ice concentrations (Arthur et al. 1996, Stirling et al. 1999, Ferguson et al. 2000, Durner et al. 2006).

The satellite PMW data used in building the RSFs had 25 × 25 km pixel resolution. However, sea ice grids among the 10 GCMs that we analyzed had various model-specific spatial resolutions ranging from about 1 × 1 to 3 × 4 degrees of latitude × longitude. To facilitate consistency among the RSF ice covariates, both with respect to the PMW covariates used to derive the RSFs and to the various GCM resolutions, we resampled the GCM grids to match the PMW grid. Each GCM native grid of sea ice concentration was converted to an Arc/Info Version 9.2 (ESRI, Redlands, California, USA) point coverage and projected to the PMW polar stereographic coordinate system. A 3-dimensional triangular irregular network (TIN; Arc/Info) was created from the point coverage using latitude, longitude, and ice concentration as the x, y, and z values, respectively, and a 25 km pixel resolution grid was generated. Effectively, this procedure over-sampled the original GCM resolution using 2D linear interpolation.

Covariates of the resource selection functions

To build and extrapolate the RSF models, we required an identical suite of covariates (predictor variables) from both the observed sea ice record and the GCM projections. Both data sources contained monthly estimates of total sea ice concentration for each 25 × 25 km pixel, which we termed totcon. Because prior RSF habitat analyses of polar bear locations and PMW data (Durner et al. 2004, 2006) showed nonlinear associations between bear distributions and totcon, we also included a second-order effect (totcon^2). We further defined three covariates based on distances to boundaries that separated ice concentration thresholds. The boundaries (or edges) separated pixels containing $\geq$15% ice, pixels containing $\geq$50% ice, and pixels containing $\geq$75% ice. From each pixel in the study area, we measured the distances to the nearest boundary pixel that partitioned each of the three ice concentration thresholds. Hence, in addition to totcon and totcon^2, each pixel in the study area (at monthly intervals) included the covariates of distances to the boundaries of $\geq$15% ice (dist15), $\geq$50% ice (dist50), and $\geq$75% ice (dist75). Spatial distributions of the ice concentration thresholds varied among seasons, but converged and were generally concordant with coastlines during winter in most of our study area (because ice concentration exceeded 75% throughout).

We included a fifth covariate which defined the distance between each pixel in the study area to the nearest coastline (dist2land). Last, we assigned ocean depth (bath) as a covariate to each pixel in the study area based on the IBCAO bathymetry chart. Therefore, each pixel, in both the data used to build the RSFs and in the data used to extrapolate the RSFs, included a total of six main effects (totcon, dist15, dist50, dist75, dist2land, and bath) and one second-order effect (totcon^2).

Defining seasons

We created four seasonal RSF models from the 1985–1995 observational record of PMW sea ice distributions and polar bear tracking data. Instead of defining seasons based on fixed intervals of calendar months, we defined four temporally dynamic seasons (maximum, melt, minimum, and growth) based on the timing and amplitude of the intrinsic annual oscillation of ice growth and melt. Our intent for classifying months into dynamic seasons was designed to accommodate future

Table 1. Extended.

RSF evaluation period (1985–1995)											
Year											
1969	1997	1998	1999	2000	2001	2002	2003	2004	2005	2006	Total
		9	4	3	49	7	21	37	50	43	223
	77	95	290	623	734	616	366	584	776	532	4693
	12	69	76	19	36	42	32	179	303	196	964
84	95	86	169								434
		5	10	247	216	335	133	261	67	43	1317
32	19	9									60
	39										39
116	242	273	549	892	1035	1000	552	1061	1196	814	7730

changes in the timing and duration of ice growth and melt when applied to the 21st-century GCM ice projections.

Our seasonal classification of any given month was determined by a threshold of sea ice change relative to the year-specific amplitude in sea ice extent (difference between the maximum ice extent and the minimum ice extent within the respective year; Fig. 2a). First, a month was assigned to the ice maximum season if that month's total ice extent in the study area (excluding East Greenland) was greater than the year-specific maximum ice extent minus 15% of the total change in annual extent (e.g., the amplitude of the annual ice-extent oscillation within the respective year). East Greenland was excluded because seasonal (melt/freeze) sea ice extent south of Fram Strait is confounded by large amounts of wind-driven ice export from the polar basin (Kwok et al. 2004). The converse of this algorithm (minimum ice extent plus 15%) was applied to classify months into the ice minimum season. Then, the remaining unclassified months (during the intervening periods) were assigned to either the ice-melt or ice-growth season depending on their chronology relative to the maximum and minimum seasons. The resulting seasonal designations throughout both the PMW and GCM periods, therefore, varied among years (Fig. 2b). Henceforth, the ice maximum, melt, minimum, and growth seasons are referred to as winter, spring, summer, and autumn, respectively.

Defining habitat available to polar bears

We were interested in the habitat choice that a bear made as it moved between two consecutive locations, hence we used pairs of consecutive locations that were separated by 4–8 days (Ferguson et al. 2000). Our procedures for estimating the RSF models were based on used habitat vs. available habitat, following the methods for discrete-choice modeling (Arthur et al. 1996, McCracken et al. 1998, Cooper and Millspaugh

Table 2. Ten Intergovernmental Panel on Climate Change (IPCC) AR-4 general circulation models (GCMs) from which sea ice simulations and projections were extracted to define ice covariates for polar bear resource selection functions (RSF) models.

Model indentification	Country of origin	Abbreviations used in this paper	Grid resolution (latitude × longitude)	Forcing scenario	Runs (*n*)
ncar_ccsm3_0	USA	CCSM3	1.0° × 1.0°	20c3m	8
				SRES A1B	8
				SRES B1	8
cccma_cgcm3_1	Canada	CGCM3 T47	3.8° × 3.8°	20c3m	1
				SRES A1B	1
cnrm_cm3	France	CNRM CM3	1.0° × 2.0°	20c3m	1
				SRES A1B	1
gfdl_cm2_0	USA	GFDL CM2	0.9° × 1.0°	20c3m	1
				SRES A1B	1
giss_aom	USA	GISS AOM	3.0° × 4.0°	20c3m	1
				SRES A1B	1
ukmo_hadgem1	UK	HadGEM1	0.8° × 1.0°	20c3m	1
				SRES A1B	1
ipsl_cm4	France	IPSL CM4	1.0° × 2.0°	20c3m	1
				SRES A1B	1
miroc3_2_medres	Japan	MIROC32	1.0° × 1.4°	20c3m	1
				SRES A1B	1
miub_echo_g	Germany/Korea	MIUB ECHO	1.5° × 2.8°	20c3m	1
				SRES A1B	1
mpi_echam5	Germany	MPI ECHAM5	1.0° × 1.0°	20c3m	1
				SRES A1B	1

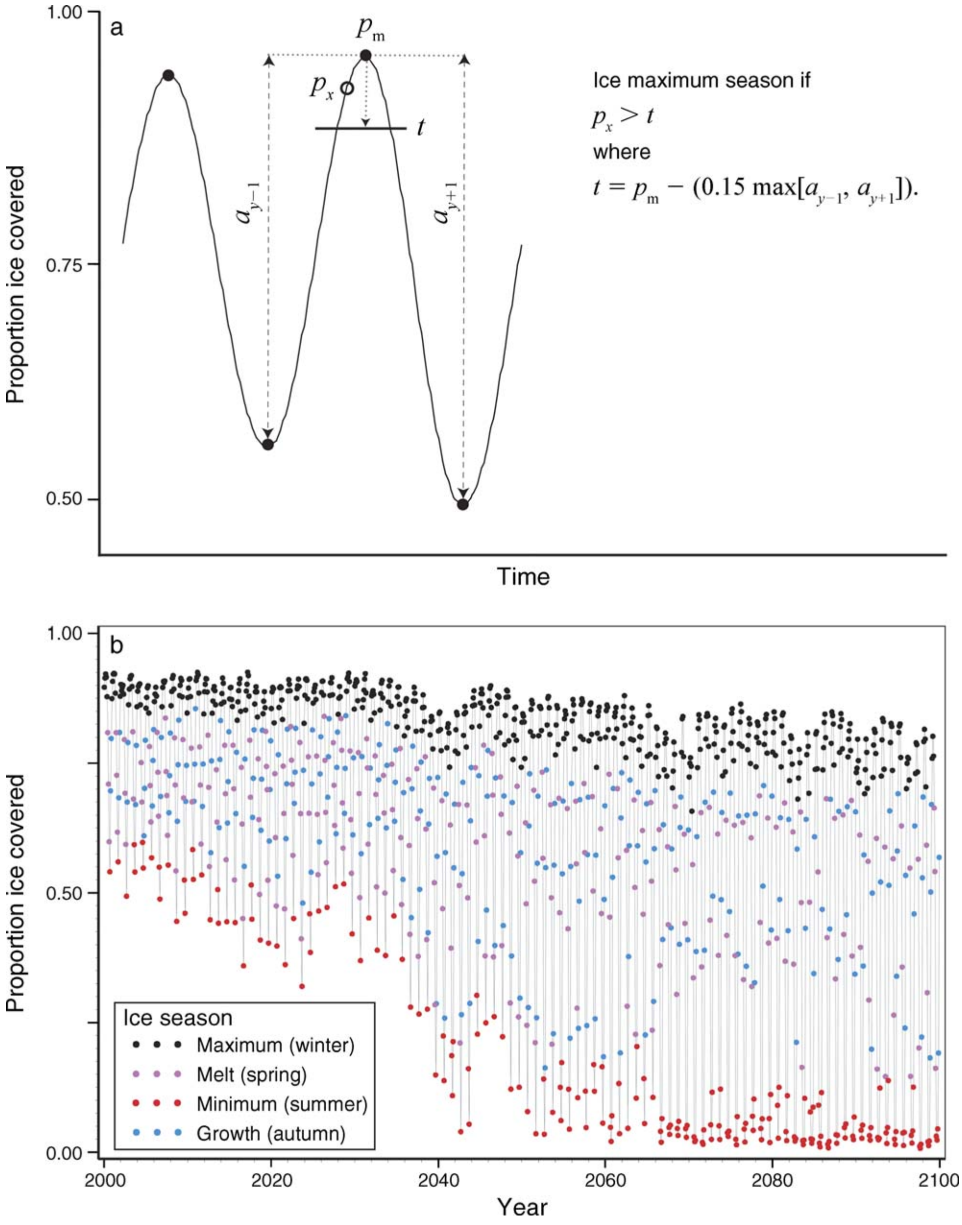

FIG. 2. (a) Schematic of the algorithm used to classify months into one of four ice-seasons. (b) Example of the ice-season classification algorithm applied to projected sea ice extent during the 21st century by the CCSM3 GCM (run-1) and the SRES-A1B forcing scenario. A month (y) was assigned to the ice-maximum season if its proportional ice extent (p_x) in the Arctic Ocean exceeded a threshold (t), as defined by the month of greatest ice extent (p_m) minus 15% of the maximum annual amplitude of ice extent change from the previous (a_{y-1}) or subsequent (a_{y+1}) minimum extent. An inverse algorithm (not shown) was used to assign months to the ice-minimum season. Intervening months were assigned to either the ice-melt or ice-growth season depending on their chronology relative to the maximum and minimum.

1999, Durner et al. 2004, 2006, Johnson et al. 2006). For each polar bear location, we defined the habitat that was available to that bear as the area within a circle, the center of which was the bear's previous location (Fig. 3a; Arthur et al. 1996, Durner et al. 2004). The radius of the circle was determined by the elapsed time between the two consecutive observations and by the distance a polar bear could travel during that time. Because movement rates of female polar bears vary by month (Amstrup et al. 2000), we calculated an expected movement rate (upper bound) for each month and a unique radius for each pair of bear locations using the following equation:

$$\text{radius of available habitat} = [a + (b \times 2)] \times c$$

where a equals the mean hourly movement rate for all bears within the respective month, b is the standard

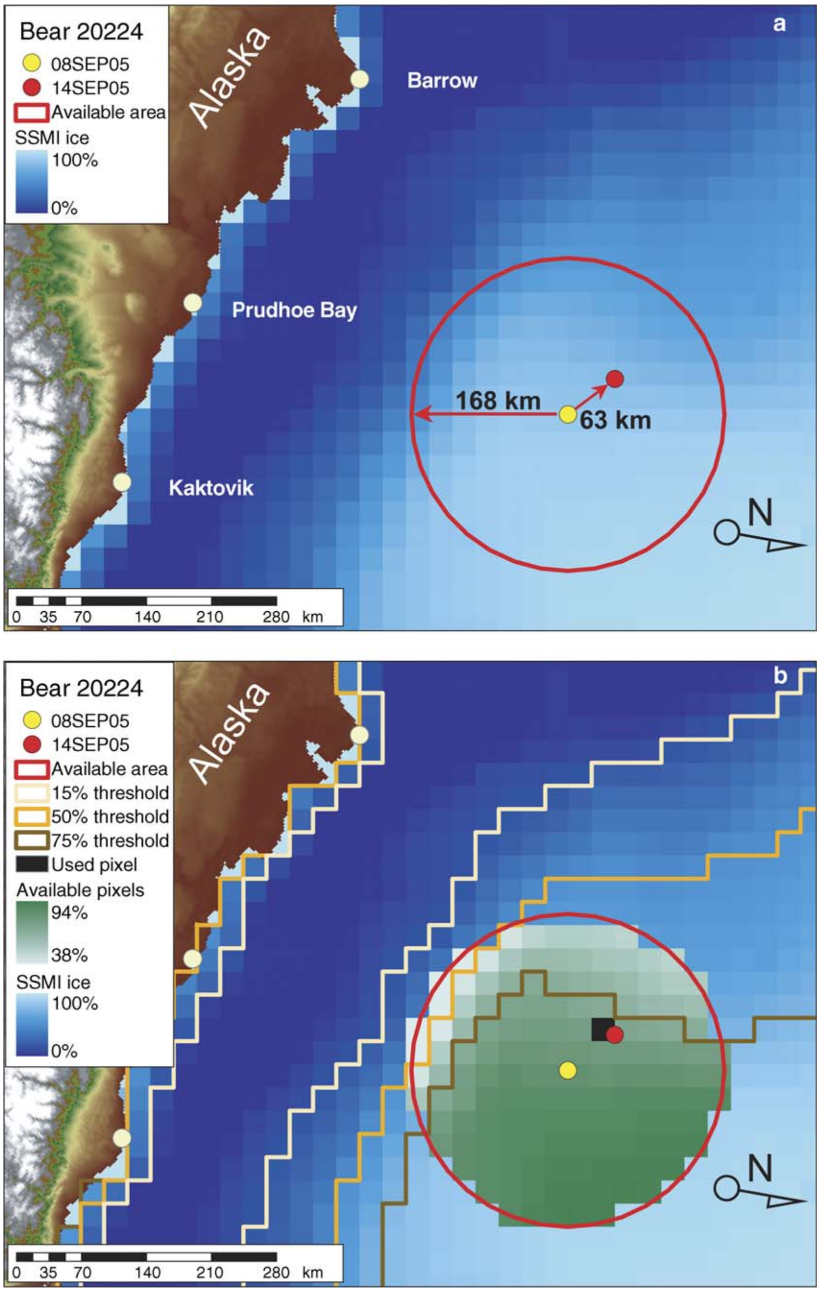

FIG. 3. (a) Example of two consecutive locations of polar bear number 20224 on the 8th (yellow point) and 14th (red point) of September 2005 and the probable extent of available habitat (red circle), had the bear sustained a maximum rate of travel for the six-day period. (b) An example of habitat pixels available to a polar bear as it moved from one location (yellow point) to a subsequent location (red point and black pixel). All pixels within the red circle were considered available for selection by the bear, but only the black pixel containing the second bear location (red point) was coded as a used point. Each pixel in the availability circle included covariates totcon, bath, dist2land, dist15, dist50, and dist75. Key to variables: totcon is a monthly estimate of the aerial extent of sea ice within each 25 × 25 km pixel; totcon^2 is the second-order effect (quadratic) of totcon; dist15 is the distance from the center of each 25 × 25 km pixel to the nearest pixel on the $\geq$15% sea ice concentration boundary; dist50 is the distance from the center of each 25 × 25 km pixel to the nearest pixel on the $\geq$50% sea ice concentration boundary; dist75 is the distance from the center of each 25 × 25 km pixel to the nearest pixel on the $\geq$75% sea ice concentration boundary; bath is ocean depth; dist2land is the distance from the center of each 25 × 25 km pixel to the nearest coastline.

TABLE 3. Candidate a priori models for a polar bear resource selection function (RSF) in the pelagic region of the Arctic, 1985–1995.

Model number	Model	Season
1	totcon	all
2	totcon + bath	all
3	totcon + dist2land	all
4	totcon + dist15	all
5	totcon + dist50	all
6	totcon + dist75	all
7	totcon + bath + dist2land	all
8	totcon + bath + dist15	all
9	totcon + bath + dist50	all
10	totcon + bath + dist75	all
11	totcon + dist2land + dist50	spring, summer
12	totcon + dist2land + dist75	spring, summer, autumn
13	totcon + dist15 + dist50	summer
14	totcon + dist15 + dist75	spring, summer, autumn
15	totcon + dist50 + dist75	spring, summer
16	totcon + totcon^2	all
17	totcon + totcon^2 + bath	all
18	totcon + totcon^2 + dist2land	all
19	totcon + totcon^2 + dist15	all
20	totcon + totcon^2 + dist50	all
21	totcon + totcon^2 + dist75	all
22	totcon + totcon^2 + bath + dist2land	all
23	totcon + totcon^2 + bath + dist15	all
24	totcon + totcon^2 + bath + dist50	all
25	totcon + totcon^2 + bath + dist75	all
26	totcon + totcon^2 + dist2land + dist50	spring, summer
27	totcon + totcon^2 + dist2land + dist75	spring, summer, autumn
28	totcon + totcon^2 + dist15 + dist50	summer
29	totcon + totcon^2 + dist15 + dist75	spring, summer, autumn
30	totcon + totcon^2 + dist50 + dist75	spring, summer

Notes: Definitions of variables: totcon is a monthly estimate of the aerial extent of sea ice within each 25 × 25 km pixel; totcon^2 is the second-order effect (quadratic) of totcon; dist15 is the distance from the center of each 25 × 25 km pixel to the nearest pixel on the $\geq$15% sea ice concentration boundary; dist50 is the distance from the center of each 25 × 25 km pixel to the nearest pixel on the $\geq$50% sea ice concentration boundary; dist75 is the distance from the center of each 25 × 25 km pixel to the nearest pixel on the $\geq$75% sea ice concentration boundary; bath is ocean depth; dist2land is the distance from the center of each 25 × 25 km pixel to the nearest coastline.

deviation of the movement rate, $\{a + (b \times 2)\}$ yields an approximation of the upper limit to the hourly movement rate, and c equals the number of hours between locations. On rare occasions, the actual straight-line distance traveled by a bear between observations exceeded the calculated radius. In these cases, the radius of available habitat was defined as the straight-line distance actually traveled.

All pixels enclosed by the resulting availability circle that consisted of sea ice were used in the RSF analysis (Fig. 3b). Durner et al. (2006) identified total ice concentration (totcon) as a critical habitat characteristic because polar bears are rarely found in open water, and a value totcon $\geq$ 15% indicated that sea ice was likely present. Therefore, only pixels within the availability circle with a sea ice estimate $\geq$15% were considered as the choice set of potential habitat for the bear as it traveled from its starting location to its ending location (coded AVAILABLE). The single pixel within the availability circle that contained the bear's ending location then represented the selected pixel (coded USED). Because the radius for each pair of locations was dependent on the elapsed time multiplied by a month-specific movement rate, the number of available pixels varied among location pairs. In summary, each choice set (AVAILABLE and USED pixels) represented a census of discrete habitat units available to a bear for the respective starting point of a location pair. Each pixel within every choice set included all six habitat covariates.

Estimating the resource selection functions

We screened the six habitat covariates (main effects) for within-season correlations before developing a set of 30 a priori RSF models (Table 3). Pairs of main effects that were strongly correlated ($|r| \geq 0.6$; Pearson's correlation coefficient; Conover 1980) within a season were not allowed in the same model. Because of the importance of sea ice to polar bears, as explained above, totcon was entered as the initial covariate in all models.

We used a discrete-choice model to estimate coefficients of each covariate and Akaike's Information Criterion for each model (AIC; Burnham and Anderson 2002). Each discrete-choice model was estimated by maximizing the multinomial logit likelihood (Manly et al. 2002). This was accomplished using the stratified Cox proportional hazards likelihood maximization routine by an adaptation of the SAS procedure PROC PHREG (SAS Institute 2000) designed to maximize the appropriate discrete choice likelihood function (Kuhfeld 2000). Standard errors of coefficients in each season were estimated by resampling, with replacement, a random subset (bootstrapping) of individual bears 2000 times.

Following the estimation of parameter values and AIC, models were ranked according to Akaike weights (Burnham and Anderson 2002) from "best" (highest Akaike weight) to "worst" within their respective seasons. Akaike weights provided a standardized AIC ranking among the suite of candidate models where the sum of model weights is 1. Relatively large increases in Akaike weights indicated large improvements between competing models. AIC rankings and weights were compared to those obtained using the Bayesian Information Criterion (BIC; Burnham and Anderson 2002), which applies higher penalties for models fit to large data sets. BIC values were calculated as $-2\ \log(L) + p[\log(n)]$, where log was the natural logarithm (base e), L was the value of the multinomial logit likelihood evaluated at the maximum-likelihood estimates, and n was the number of choice sets, or polar bear locations. Final RSF predictions of habitat selection involved model averaging within each season (Burnham and Anderson 2002), unless the AIC or BIC weights suggested there was only one reasonable model. Each a priori model within a season was used to predict every pixel's relative probability of selection (use by a polar bear), and a weighted mean probability was computed across all models based on their AIC weights.

Assessing the resource selection functions

We applied an empirical method to assess performance of each final RSF by comparing the RSF values of pixels selected by polar bears (used pixels) to the range of RSF values throughout the study area. Monthly RSF-value maps were constructed by applying the appropriate RSF seasonal model (depending on the respective month's seasonal classification as described above) to every ice-covered pixel throughout the study area based on each pixel's individual habitat covariates. Each monthly RSF-value map was projected to an equal area projection (Lambert Azimuthal) and partitioned into 20 equal area zones along an increasing RSF-value gradient. In other words, each zone represented 5% of the available habitat across the study area (in the respective month), and the zones were labeled 1–20, with 20 representing the zone of highest relative RSF value. Each polar bear location ($n = 19\,901$; 1985–2006) was intersected with its respective monthly map of equal area RSF zones and associated with the zone-number occupied. Frequencies of polar bear occupancy within the 20 zones were evaluated against the null expectation that occupancy would be equivalent among the 20 zones if polar bears exhibited no selection preference among the six habitat covariates.

Extrapolating monthly RSF maps

Twelve monthly RSF-value maps were generated annually using the season-specific RSF model that corresponded with each month's seasonal classification. RSF values (the relative probability of polar bear utilization) were calculated for each 25 × 25 km study-area pixel based on its respective habitat covariates. Monthly RSF maps were created for (1) the observed PMW sea ice record (1979–2006), (2) the late 20th-century ice simulations by each of the 10 GCMs (~1950–2000), and (3) the 21st-century ice projections by each of the 10 GCMs (2000–2100). A total of 39 360 monthly RSF-value maps were created from the full suite of observed and modeled (Table 2) sea ice data sets.

Defining optimal polar bear habitat

The RSF represents the relative probability of use of a resource unit and it is proportional to the exponential linear function of the covariates. Magnitudes of RSF values are established by the unique combination of covariates and coefficients that comprise the specific models. Therefore, raw RSF values generated by a model for one season (e.g., spring) cannot be compared directly to or combined with those generated by a model for another season (e.g., winter). To assess annual changes in polar bear habitat over time, we needed to develop a common metric that allowed the information in RSF values to be pooled, regardless of the model generating them. We did this by establishing a season-specific RSF threshold that distinguished "optimal" habitat (based on observational data) from non-optimal habitat.

Histograms of all polar bear location data gathered between 1985 and 1995 revealed that at least 70% of bear locations consistently occurred in the upper 20% of RSF-valued area. We defined optimal habitat, therefore, as the mean RSF value that separated the upper 20% from the lower 80% of the RSF-valued area for each season. All mapped pixels with raw RSF values greater than the upper 20% threshold, therefore, were included in optimal habitat. In this way we converted RSF values, which cannot be pooled, to the number of square kilometers of mapped pixels of optimal habitat, which can be pooled.

We pooled the outputs of the four seasonal RSF models into an annual metric by extracting the monthly area (km^2) of optimal habitat, and summing the 12 monthly areas to arrive at a cumulative annual area of available optimal habitat. The cumulative annual area of optimal habitat was calculated within each subpopulation and subpopulation group (Fig. 1) for all years of the observed satellite sea ice record, as well as the late 20th-century hindcast simulations and 21st-century ice projections by the 10 GCMs (Table 2).

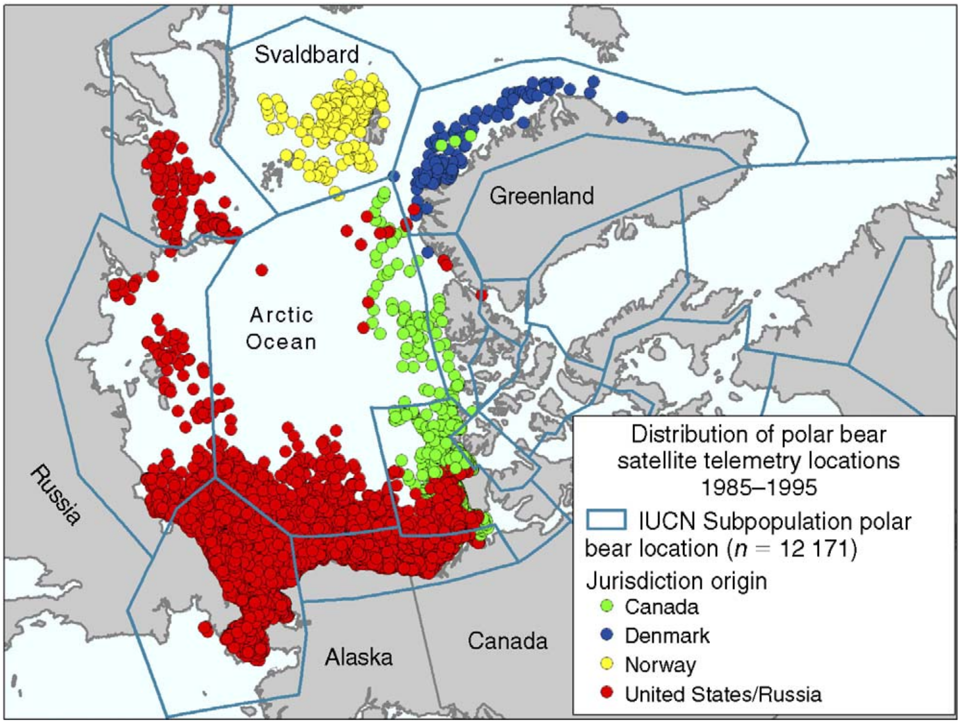

FIG. 4. Distribution of all polar bear locations 1985–1995, by jurisdictional origin, used to build polar bear resource selection functions (RSF) for the pelagic realm of the Arctic.

We expressed 21st-century changes in the amount of optimal habitat as percentage change relative to the 1985–1995 baseline habitat. We emphasize that our four seasonal thresholds, derived from the 1985–1995 period, remained fixed. Thus, when we extracted the area of optimal habitat from the 21st-century maps of RSF, the threshold values remained those that were observed in 1985–1995. This approach created a foundation that allowed us to examine whether future ice projections indicated increases, decreases, or stability in the cumulative annual area of optimal polar bear habitat, relative to the earliest decade of empirical observations. Inherently, this approach assumes that, given the opportunity, polar bears in the future will select habitats in the same way they did between 1985 and 1995, despite potential dramatic seasonal changes in ice extent and distribution.

Quantifying changes in polar bear habitat

Absolute and percentage-change metrics of sea ice extent, RSF value, and optimal habitat area were used to quantify 20th- and 21st-century changes and trends in the study area. Changes were examined temporally within individual subpopulations, groups of subpopulations, and for the study area as a whole (Fig. 1). We also assessed variability among GCMs in their projections of sea ice cover and polar bear habitat. We used linear least squares regression to examine rates of change in the area of optimal habitat. Analyses were conducted for the 21st century as a whole and on selected decadal time periods.

RESULTS

Polar bear location data

The 1985–1995 polar bear location data used to construct the RSF models were distributed throughout the study area (Fig. 4); however, sample sizes varied considerably among subpopulations (Table 1). Over 66% of the polar bear locations available for estimating RSFs were from the Chukchi Sea and Southern Beaufort Sea. Bear locations in the Laptev Sea and the Arctic Basin made up an additional 25%. The total number of collared bears and bear locations used for estimating seasonal RSFs was greatest in winter and lowest in autumn (Table 4). A total of 12 171 used and 1 310 805 available habitat records comprised the 1985–1995 data set, and 7730 used and 722 405 available records comprised the 1996–2006 data set.

Seasons

Defining seasons based on changes in ice extent rather than calendar-month intervals resulted in modest annual variation and trends in seasonal chronology and duration. Within the full observational period (1985–2006), winter began in November (2 years), December (7 years), or January (2 years), and continued to April (1 year) or May (10 years). Spring began in May (1 year) or June (10 years) and continued to July (9 years) or August (2 years).

TABLE 4. Data distribution of individual polar bears and number of used locations used to build a polar bear resource selection function for the pelagic realm of the Arctic, 1985–1995.

Season	Number of individuals	Number of used locations
Winter	322	5488
Spring	292	3408
Summer	237	1650
Autumn	216	1625
Total	N/A	12 171

Note: Location data from most bears occurred in more than one season. "N/A" indicates "not applicable" because we did not build a "full year" RSF model. We can sum the total number of locations, because each unique location can only appear in one season, but we cannot sum the total number of bears because each individual bear usually appeared in more than one season.

Summer was represented by August and September (9 years) or by September only (2 years). Autumn always began in October, often included November (9 years), and rarely included December (2 years).

The mean length of seasons over the 21st century remained generally unchanged (Fig. 5). Overall, for both the observed and modeled ice data, duration of winter averaged ~6 months and other seasons averaged ~2 months each. There was a slight increase in mean length of the summer season during the latter half of the 21st century caused by a few GCMs that projected nearly ice-free summers, such as run-1 for CCSM3 (Fig. 2b), where the number of months composing the summer season increased after about 2065. Longer summer seasons were typically reflected by shorter winter seasons (i.e., the length of spring and autumn remained unchanged throughout the 21st century).

Resource selection functions

Correlations between RSF covariates (Pearson's $|r| > 0.6$; Table 5) reduced the number of candidate RSF models. Twenty models were estimated for winter, 28 for spring, 30 for summer, and 24 for autumn (Table 3). The top models for every season had AIC and BIC weights >0.99. Therefore, the pooled contribution from all models within a season was heavily weighted by the covariate estimates of the best model, so model averaging was effectively inconsequential and omitted. The top model for the winter season contained totcon, totcon^2, bath, and dist2land (Table 6). The top models for the remaining seasons all contained totcon, totcon^2, bath, and dist15 (Table 6).

Despite overall similarity among the four seasonal RSF model structures, differences in the magnitude of the parameter estimates indicated that there were seasonal differences in polar bear habitat selection (Fig. 6). Standardized plots of relative selection probability, assuming all other variables were held constant at their respective medians, showed that selection decreased with increasing values of bath, dist2land, and dist15. Owing to the totcon quadratic in each model, the relative probability of selection peaked at total ice concentrations of 95%, 80%, 65%, and 60% for winter,

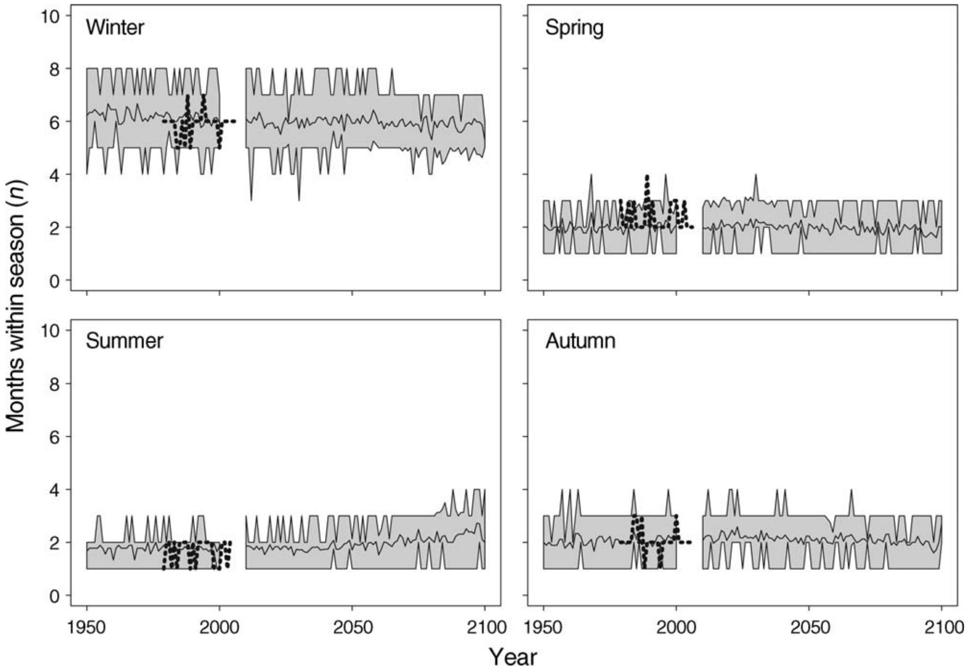

FIG. 5. Ensemble mean season length of 10 general circulation models (GCMs) used in this study (black line, mean ± min/max) and the observed satellite record (dotted line), where seasons were dynamically defined by the amplitude of annual ice growth and retreat (see Fig. 2).

TABLE 5. Pearson correlation matrix of covariates used for a polar bear resource selection function (RSF) in the pelagic realm of the Arctic, 1985–1995.

	Variable 2					
Variable 1	totcon	dist2land	bath	dist15	dist50	dist75
Winter						
totcon	1					
dist2land	0.015	1				
bath	0.082	0.443	1			
dist15	0.200	0.763†	0.234	1		
dist50	0.208	0.778†	0.249	0.975†	1	
dist75	0.158	0.753†	0.266	0.948†	0.977†	1
Spring						
totcon	1					
dist2land	0.125	1				
bath	0.204	0.365	1			
dist15	0.427	0.656†	0.234	1		
dist50	0.252	0.512	0.214	0.812†	1	
dist75	−0.391	0.232	0.023	0.236	0.480	1
Summer						
totcon	1					
dist2land	0.350	1				
bath	0.405	0.344	1			
dist15	0.520	0.609†	0.401	1		
dist50	−0.097	0.209	0.027	0.585	1	
dist75	−0.537	−0.176	−0.184	−0.040	0.515	1
Autumn						
totcon	1					
dist2land	0.162	1				
bath	0.254	0.424	1			
dist15	0.342	0.708†	0.303	1		
dist50	0.307	0.600†	0.375	0.751†	1	
dist75	−0.095	0.396	0.264	0.442	0.754†	1

Note: Covariates are defined in Table 3.
† Correlation > 0.6.

spring, summer, and autumn, respectively, and then declined with further increases in concentration.

Selection for shallow water was strongest in the winter, and weakest in the summer (Fig. 6). During winter, for example, the standardized RSF value for 1300 m depth was 0.6, but an equivalent RSF value did not occur in summer until depths of 3000 m. Polar bears showed strongest selection for the 15% sea ice concentration threshold in autumn, reduced selection in summer, and lowest selection in spring (Fig. 6). During winter, distance to land was a stronger covariate than distance to the 15% sea ice concentration threshold; but because these two covariates were highly correlated in winter ($r = 0.76$; Table 5), they may be considered partly equivalent.

Resource selection function assessment

Frequency distributions of observed polar bear locations within equal-area RSF intervals resembled an exponential function, confirming the final RSFs pos-

TABLE 6. Coefficients and standard errors (in parentheses) of covariates in the top model for each season for resource selection functions for polar bears in the polar basin.

Season	totcon	totcon^2	bath	dist2land	dist15
Winter	0.08602	−0.00046	−0.00037	−0.00474	
	(0.01856)	(0.00012)	(0.00006)	(0.00047)	
Spring	0.06551	−0.00040	−0.00020		−0.00261
	(0.00409)	(0.00004)	(0.00005)		(0.00050)
Summer	0.04676	−0.00037	−0.00017		−0.00436
	(0.00582)	(0.00007)	(0.00005)		(0.00083)
Autumn	0.08130	−0.00068	−0.00025		−0.00604
	(0.00635)	(0.00006)	(0.00005)		(0.00054)

Notes: Standard errors (in parentheses) were calculated by bootstrapping (replicates = 2000) individual bears. Among all the seasons, the best models included a total of five covariates. Within each season, however, the best model included only four covariates. Hence, in winter, dist15 was not selected for inclusion in the best winter model but was selected for spring, summer, and autumn. Likewise, dist2land was selected in the best winter model but was not selected for inclusion in the best spring, summer or autumn model. Covariates are defined in Table 3.

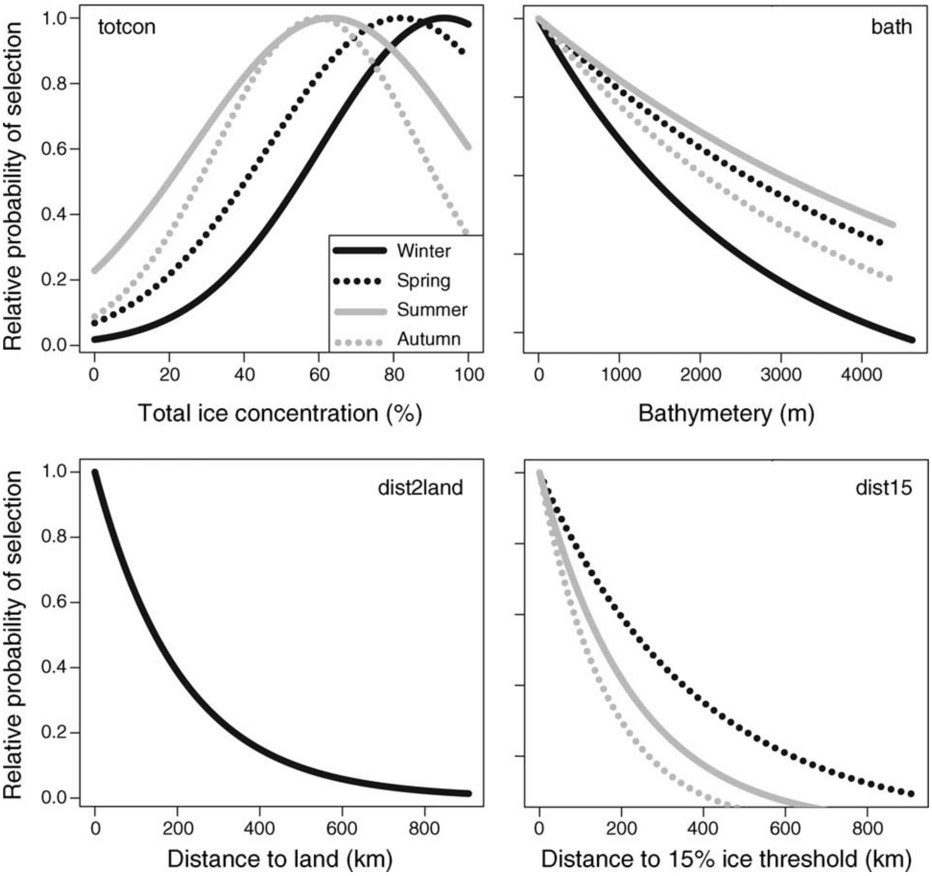

FIG. 6. Responses of four covariates in the seasonal resource selection function (RSF) models developed for polar bears in the pelagic realm of the Arctic, 1985–1995. Variables not in plots were held at their median values. RSF predictions were scaled so the maximum prediction was 1.0 for each season.

sessed the hypothesized ability to distinguish habitat selection (Fig. 7). During 1985–1995 and 1996–2006, 71.2% and 82.3% of polar bear locations, respectively, occurred in the upper 20% of the RSF-valued habitat area (the four highest-valued RSF equal area intervals). The upper 20% of RSF-valued habitat area encompassed a majority (>70%) of polar bear locations, so (as described earlier) we used the 1985–1995 mean lower bound of the 17th (of 20) 5% equal-area interval in each season to distinguish pixels of "optimal" polar bear habitat from all other season-specific RSF pixels in all other years.

When data were pooled among all seasons and years (1985–2006), RSF performance remained strong in both the Divergent and Convergent ecoregions (Table 7). Sixty-seven percent and 87% of polar bear locations occurred within the upper 20% of RSF-valued habitat for the Divergent and Convergent ecoregions, respectively. RSF performance, however, varied among subpopulations. Performance was generally low in subpopulations of the marginal seas of the Eurasian continental shelf (Kara Sea, 43%), but was more robust in the Barents Sea (72%) and the subpopulations bordering North America (southern Beaufort Sea, 64%). Despite this variation, the top 50% of RSF-valued habitats was occupied by a substantive majority (≥70%) of the polar bear locations in all subpopulations (Table 7).

Resource selection function maps

Individual monthly RSF maps represent the basic elements we used for assessing future habitat changes and trends, so it is beneficial to illustrate their content and highlight a few general patterns in RSF habitat distributions, seasonal trends, and variability among the GCMs (Fig. 8). First, it is apparent in Fig. 8 that higher value RSF habitat occurs mainly around the peripheral shelf waters of the polar basin and never in the deep-water central basin, largely owing to the negative effect of the bathymetry covariate (Fig. 6). Second, comparing a representative summer month (September 1985) from the early decade (1985–1995) to a recent month of record minimum ice extent (September 2005) exemplifies the losses of summer habitat that polar bears have already experienced, especially in most areas of the Divergent ecoregion (Fig. 8a). Third, there is consider-

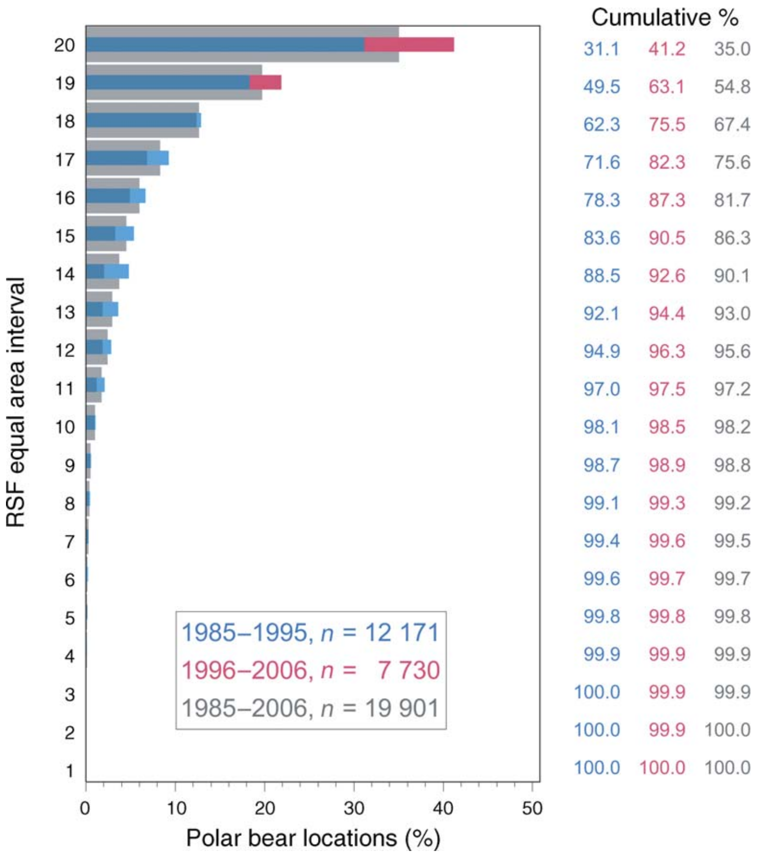

FIG. 7. Proportions of polar bear tracking locations occupying 20 equal area intervals of the extrapolated monthly resource selection function (RSF) maps (i.e., each 5% of the total monthly RSF habitat) along an increasing RSF-value gradient. All locations (gray histograms and cumulative frequencies) are shown partitioned into the 1985–1995 period (light blue) that was used to estimate the RSF models, and the subsequent 1996–2006 period (red) when sea ice conditions were markedly different and tracking studies were conducted primarily in the Beaufort Sea. Histogram segments appear dark blue when the 1985–1995 and 1996–2006 proportions overlap.

able variability among the 10 GCMs in their projections of summer habitat extent and distribution during the mid- and late-21st century (Fig. 8b); and fourth, habitat changes are far less pronounced and less variable among GCMs during winter (Fig. 8c).

Twenty-first century habitat trends

To understand trends in polar bear habitat, it is helpful to first consider the general trends projected for sea ice. All 10 GCMs simulate a downward trend in sea ice extent, with a more pronounced downward trend during summer (Fig. 9a). Even in the CCSM3 ice projections based on the SRES-B1 scenario (forcing scenario with less greenhouse gas loading), sea ice was projected to diminish, albeit less rapidly (CCSM3 B1 in Fig. 9a). Despite overall agreement in the direction of change, the 10 GCMs varied in the estimated amount of total ice extent and rate of change.

Compared to observations, the GCM-ensemble mean overestimates ice extent in the study area in both the late-20th century simulations and the early-21st century projections (Fig. 9a). Furthermore, the recent rate of

TABLE 7. Regional assessment of resource selection function (RSF) model performance for all seasons (pooled) and years (1985–2006) showing the proportion of polar bear locations within the top 20% and top 50% of the RSF-valued habitat.

Region	In the top 20% RSF-valued habitat	In the top 50% RSF-valued habitat	Number of polar bear locations
Full study area (i.e., Fig. 7)	76%	97%	19 901
Divergent ecoregion	67%	90%	14 408
Convergent ecoregion	87%	99%	5493
Arctic Basin	97%	100%	2308
Northern Beaufort Sea	77%	99%	2959
East Greenland	50%	88%	198
Queen Elizabeth	79%	100%	28
Southern Beaufort Sea	64%	94%	8455
Chukchi Sea	47%	85%	4536
Laptev Sea	47%	75%	297
Kara Sea	43%	70%	168
Barents Sea	72%	87%	952

Note: The total monthly RSF habitat area of each region was independently partitioned into 20 equal-area RSF-value intervals prior to enumerating the within-interval bear frequencies.

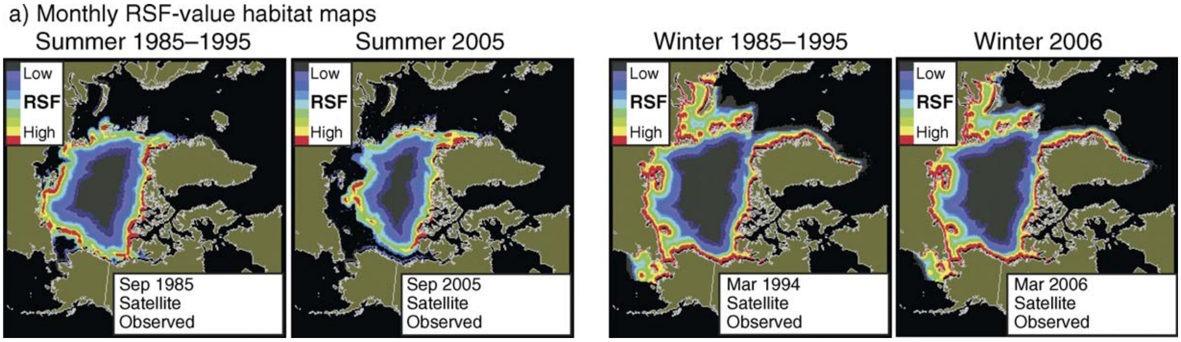

FIG. 8. (a) Examples of monthly resource selection function (RSF) value habitat maps derived from satellite-observed sea ice data with the summer RSF model and the winter RSF model. To represent a single month within the 1985–1995 period, the year-month with the smallest difference in ice extent compared to the decadal mean was selected for illustration. The year 2005 is shown to illustrate observed changes in a recent record-breaking year of minimum summer ice extent. (b) Examples of monthly summer RSF-value habitat maps for the mid- and late-21st century derived with ice projections by 10 IPCC AR-4 generalized circulation models (GCMs; labeled in lower right corner of each panel) when forced with the SRES-A1B scenario. To represent a decadal range of years, the year-month with the smallest difference in ice extent compared to the decadal mean was selected for illustration. (c) Examples of monthly winter RSF-value habitat maps for the mid- and late-21st century derived with ice projections by 10 IPCC AR-4 GCMs (labeled in lower right corner of each panel) when forced with the SRES-A1B scenario. Again, to represent a decadal range of years, the year-month with the smallest difference in ice extent compared to the decadal mean was selected for illustration.

summer ice decline based on observations is steeper than that of the GCM ensemble mean during the early 21st century. For the present study, however, we are more interested in the amount of change that is projected by the GCMs and less about accuracy of any one GCM's initial estimate. Therefore, we calculated each model's percentage change relative to itself (Fig. 9a, right). Baselines for calculating percentage change used the 1990–1999 mean for the observed ice record and the 20th-century ice simulations, and the 2001–2010 mean for the 21st-century projections. The GCM ensemble mean indicated an ~75% loss in summer ice extent by the end of century, with the greatest rate of loss during mid-century. By contrast, the projected percentage change in winter ice extent is notably smaller and much more consistent among the GCMs.

A strong association between total ice extent and total RSF habitat value is apparent within the study area (Fig. 9b). Reduced ice cover infers less overall value in available polar bear habitat because the spatial pattern of ice melt is generally from the southern ice margin poleward (i.e., coastal and shelf water habitats are melting first). All GCMs overestimated the sum total of summer RSF habitat value when compared to values calculated from observational data, and most GCMs overestimated the winter RSF habitat value. The GCM ensemble mean shows that ~60% of the sum of summer RSF habitat value is lost by the year 2100. The CCSM3 B1 forcing scenario projected RSF habitat value to decline to ~45% of pre-2000 levels (Fig. 9b). Similarity in the sum total of winter RSF habitat value between the observed and projected time periods indicates there will be relatively little change in the future amounts of higher-valued polar bear habitats during winter.

Projected rates of change in cumulative annual area of optimal polar bear habitat during the 21st century varied considerably among the IUCN units and grouped units (Fig. 10). Within the Divergent ecoregion (Fig. 10a), rates of decline are projected to be greatest in the Southern Beaufort, Chukchi, and Barents Sea subpopulations. By comparison, little change, or even slight increases in habitat, are projected for the Queen Elizabeth and Arctic Basin subpopulations in the Convergent ecoregion (Fig. 10b). Very little optimal habitat, however, existed in the Arctic Basin to begin with (12-month sum of 18×10^3 km^2 compared to 985×10^3 km^2 in the Southern Beaufort Sea), so the positive percentage change represents only a small increase in actual habitat area. The CCSM3 projections by the B1 forcing scenario were often similar to the ensemble mean until about 2030 (Fig. 10a, b).

Net annual habitat changes were characterized by dramatic losses during summer, ameliorated by relatively little change during the long winter season (Fig. 11). Over the full study area (Fig. 11a), projected losses of annually integrated optimal habitat ranged from 17% in the decade of 2045–2054 to 32% in the decade of 2090–2099. When considered seasonally, declines in optimal habitat were greatest during spring and summer. Projections of spring and summer optimal habitat declines were 36% and 42% in the decade of 2045–2054, and 55% and 68% in the decade of 2090–2099, respectively. Autumn declines for the same time periods, 21% and 27%, were intermediate between winter and summer. Because little change is predicted for half of the year (winter), average annual habitat losses in the range of 30% (Fig. 11a) translate to spring and summer losses that are about two times greater.

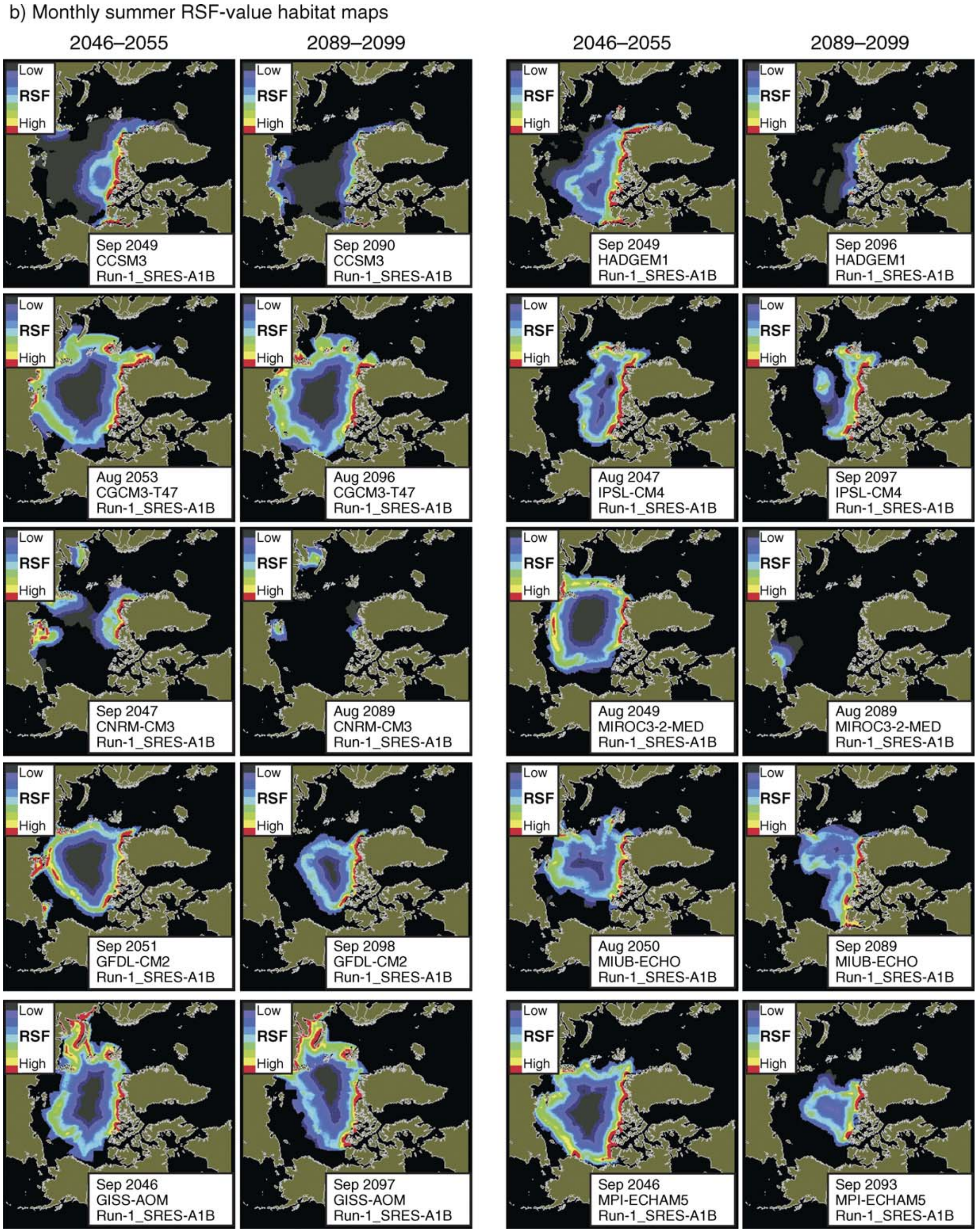

FIG. 8. Continued.

Habitat losses were more pronounced in spring, summer, and autumn in the Divergent ecoregion compared to the Convergent ecoregion, especially during the autumn season (Fig. 11b, c). The Divergent ecoregion was projected to lose 60–80% of the polar bears' historical area of spring and summer habitat by the end of the century (Fig. 11b). The Convergent ecoregion (Fig. 11c) has historically contained less total

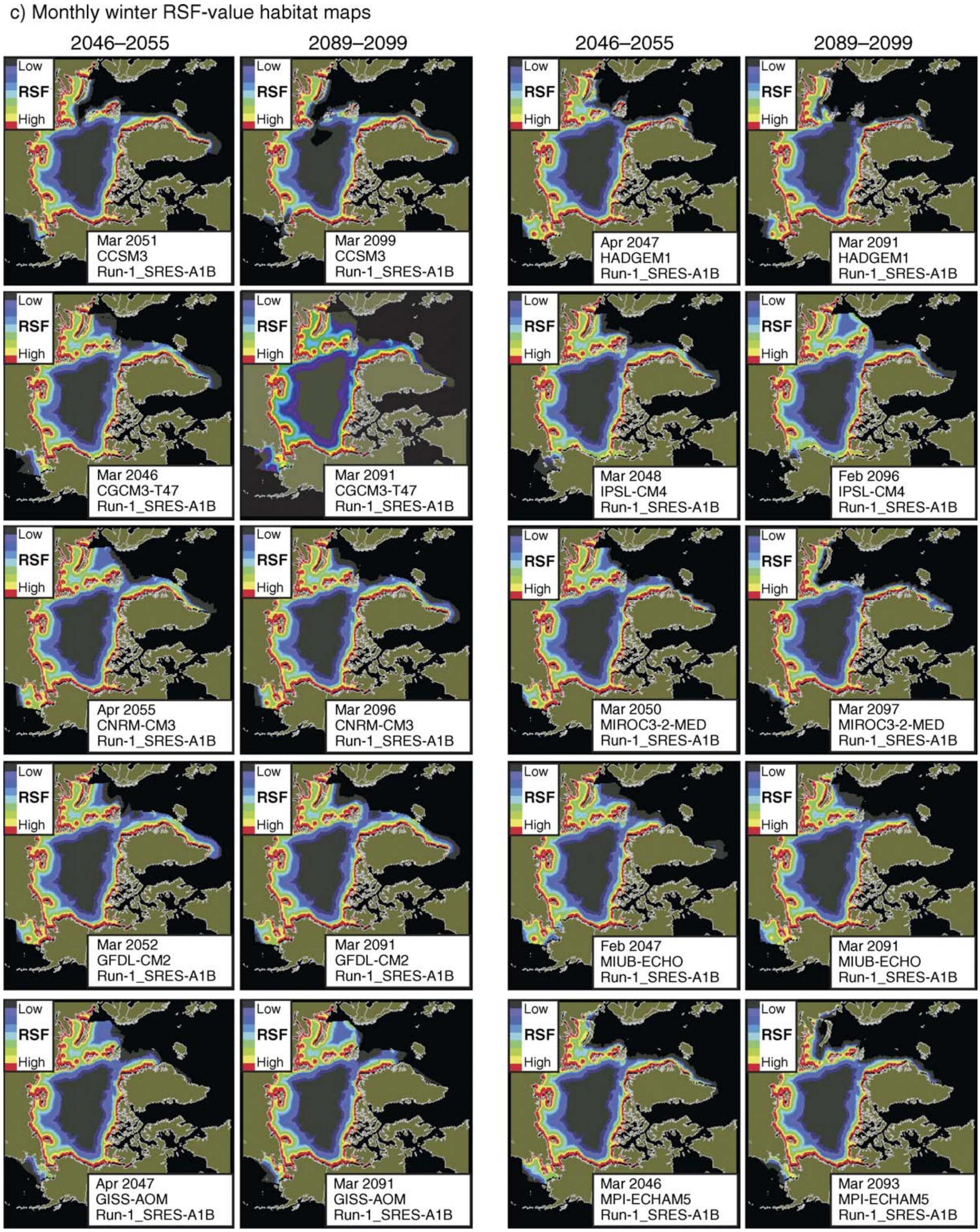

FIG. 8. Continued.

optimal habitat area, primarily because it is a smaller geographic area than the Divergent ecoregion. Nevertheless, while there is a similar seasonal pattern to the projected losses of optimal habitat, the magnitude is much less owing to the predicted relative stability of ice in the Queen Elizabeth region (Fig. 10b).

Projected rates of habitat loss over the 21st century are not constant over time (i.e., they were nonlinear;

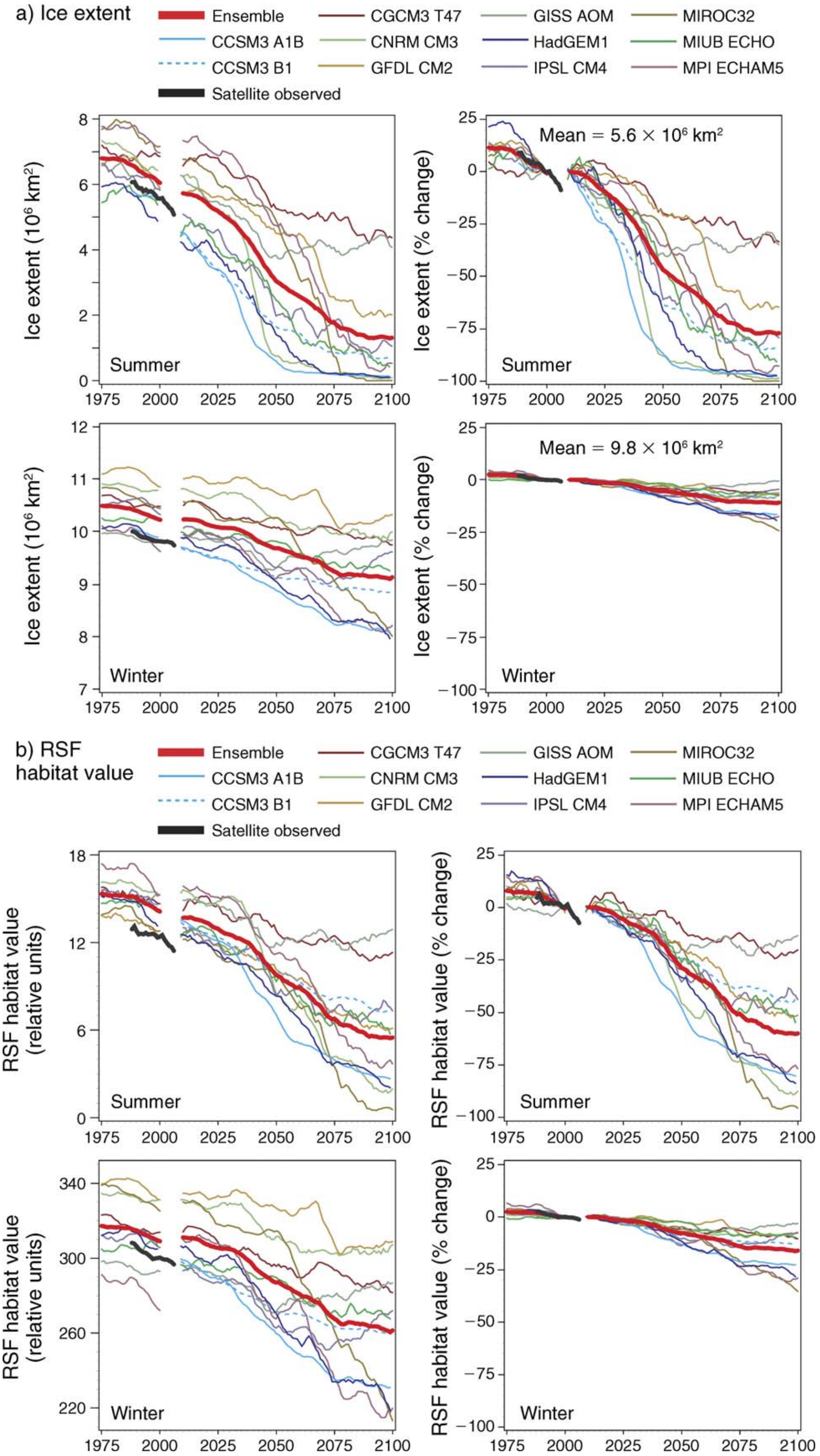
a) Ice extent
Ensemble
CGCM3 T47
GISS AOM
MIROC32
CCSM3 A1B
CNRM CM3
HadGEM1
MIUB ECHO
CCSM3 B1
GFDL CM2
IPSL CM4
MPI ECHAM5
Satellite observed
Ice extent (10^6 km^2)
Ice extent (% change)
Mean = 5.6 × 10^6 km^2
Summer
Mean = 9.8 × 10^6 km^2
Winter
1975
2000
2025
2050
2075
2100
b) RSF habitat value
RSF habitat value (relative units)
RSF habitat value (% change)
Summer
Winter

Fig. 12a–c). Rates of loss tend to be greatest during the second and third quarters of the century and then diminish during the last quarter (Figs. 9 and 10). Losses in optimal habitat from 1985 through 1995 to 1996 through 2006 establish an observed trajectory of change that is remarkably consistent with the GCM projections.

There were significant rates of change in the cumulative area of optimal sea ice habitat in the 21st century for most subpopulations, the two ecoregions, and the study area as a whole (Table 8). The sole exception was in the Arctic Basin, where there was a significant 1.6% per decade increase (Table 8). The small absolute amount of habitat change in the Arctic Basin, however, was inconsequential to overall net changes basin-wide. The mean rate of optimal habitat change for the entire study area was approximately −4% per decade. Decreases ranged from −0.9% (Queen Elizabeth) to −6.5% (Barents Sea) per decade. Notably, four of the 10 GCMs (CCSM3, HadGEM, MIROC, and MPI) projected near depletion of all optimal habitat (year round) in the Barents Sea.

Spatial changes in optimal polar bear habitat

Declines in optimal polar bear habitat between the early (1985–1995) and later decades (1996–2006) of the observational record varied spatially across the study area (Fig. 12). Large declines in optimal habitat occurred in the Southern Beaufort, Chukchi, Barents, and East Greenland seas, while offsetting patches of habitat gain and loss resulted in little net change in the Laptev, Kara, Northern Beaufort, and Queen Elizabeth subpopulations. As there was little optimal habitat in the Arctic Basin during 1985–1995 ($<13\,000$ km^2 when summed over 12 months), the relatively small increase of $\sim$11 000 km^2 translated to a large percentage ($\sim$83%) increase. By comparison, the Southern Beaufort Sea experienced a much larger net loss ($\sim$64 000 km^2, −6.2% change) of optimal habitat between 1985–1995 and 1996–2006.

Projected changes in polar bear habitat throughout the 21st century (Fig. 13) showed continuity with those already observed at the century's onset (Fig. 12). The 21st-century projections indicate that the greatest proportional losses of optimal habitat will continue to occur in the Chukchi, Southern Beaufort, Barents, and East Greenland seas. Dramatic losses of optimal polar bear habitats are projected to occur around all coastal regions of the polar basin except the Queen Elizabeth region of the Canadian Arctic (Fig. 13) where optimal habitat area is likely to be largely sustained (Fig. 10).

DISCUSSION

Resource selection functions

Our results confirm that habitat selection by polar bears can be modeled by coarse-grain environmental features. Despite a large seasonal variation in sea ice extent and composition, all four seasonal RSFs included the same, or functionally similar, habitat covariates. While the general response to any specific habitat covariate was similar among seasons, the magnitudes of the covariate parameter estimates varied among the seasonal models. This suggests that while the same habitat covariates are important throughout the annual cycle, their effects were seasonally dependent.

Previous studies of polar bear habitat relationships have confirmed that total amount, composition, and type of sea ice (or the lack thereof) function as the ultimate factors that influence polar bear spatial and seasonal movement patterns (Stirling et al. 1993, Arthur et al. 1996, Ferguson et al. 1997, 2000, Mauritzen et al. 2001, Durner et al. 2004, 2006). The polar bears analyzed for this study almost exclusively occupied pelagic regions. During the summer, when sea ice extent was at its annual minimum, most polar bears within the study area remained on the ice rather than retreating to land. It was reasonable, therefore, to include sea ice concentration in all of the a priori models for each season.

The RSF models were constructed to collectively quantify habitat selection by all polar bear populations throughout the polar basin. More than 70% of polar bear locations occurred within the highest 20% of RSF-valued habitat (Fig. 7), thus confirming that the RSF models successfully emulated the basin-wide distribution of polar bears. There was consistent RSF performance between the two observational periods, 1985–1995 and 1996–2006, even though the later period included some of the most extreme melt seasons since 1979. Pooling the polar bear tracking data from throughout the Arctic obviously strengthened robustness of the RSF models for basin-wide application. At regional scales, however, numerous factors may cause performance of the models to vary (Overland and Wang 2007): (1) seasons are not synchronous between regions (Belchansky et al. 2004); (2) a single suite of RSF covariates cannot entirely

←

FIG. 9. (a) Mean monthly ice extent in the full study area during the summer and winter ice seasons (left column) and expressed as percentage change (right column) relative to the respective model's 1990–1999 mean for the 20th-century hindcasts and the satellite-observed record and the 2001–2010 mean for the 21st-century GCM projections. (b) Mean monthly resource selection function (RSF) habitat value (relative units of probability) summed throughout the study area during the summer and winter ice seasons (left column) and expressed as percentage change (right column) relative to the decadal means defined above. Mean monthly values of ice extent (panel a, right column) during 1990–1999 from the satellite observed record are shown in the ice-extent percentage-change panels to provide a baseline for assessing the effective magnitude of change. All results are plotted as 10-year running means. Results for CCSM3 run under the B1 forcing scenario are shown with a dashed line.

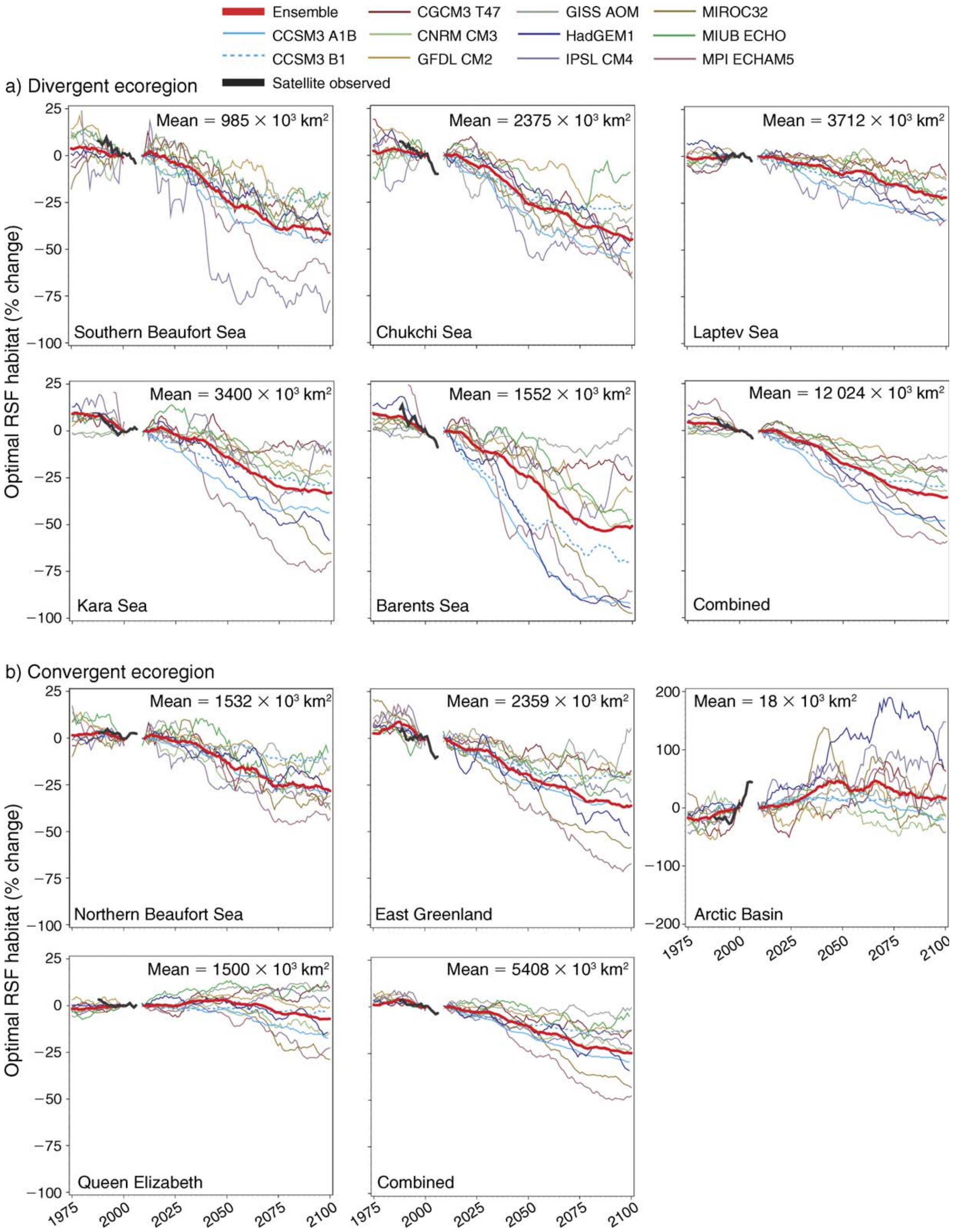

FIG. 10. (a) Percentage change in the total annual (12 month) area of optimal polar bear habitat in the IUCN units of the Divergent ecoregion, plotted as 10-year running means. (b) Percentage change in the total annual (12 months) area of optimal polar bear habitat in the Conservation of Nature and Natural Resources (IUCN) units of the Convergent ecoregion, plotted as 10-year running means. Note that the *y*-axis is scaled differently for the Arctic Basin unit. For both ecoregions, results for CCSM3 run under the B1 forcing scenario are shown with a dashed line. The mean annual total area of optimal habitat (10^3 km^2) during 1990–1999 from the satellite observed record is shown to provide a baseline for assessing the effective magnitude of the percentage change.

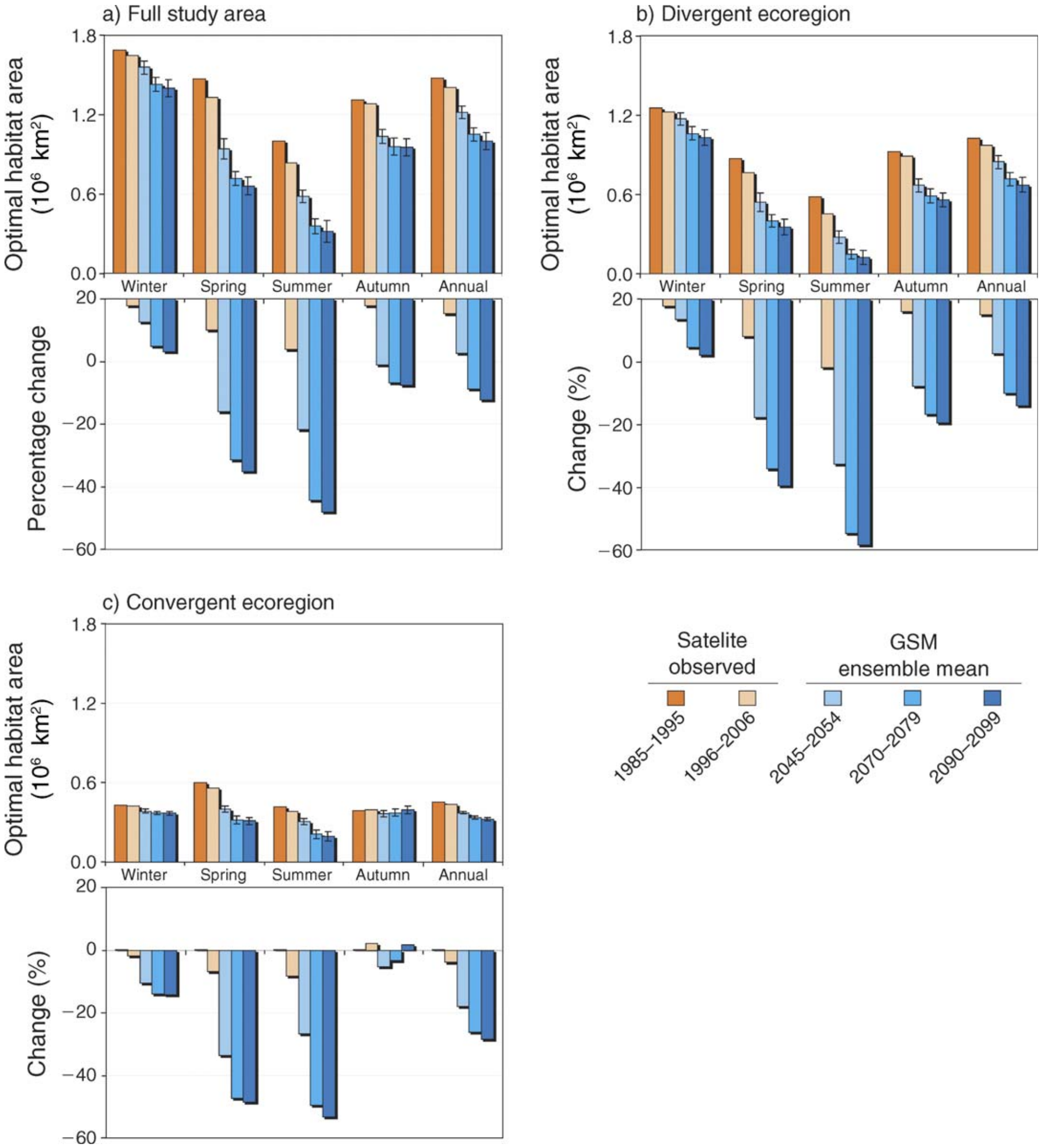

FIG. 11. (Upper histograms) Mean area of optimal polar bear habitat in the (a) full study area, (b) Divergent ecoregion IUCN group, and (c) Convergent ecoregion IUCN group during two decadal periods of the satellite observed sea ice record and three decadal periods of the 21st century based on sea ice projections by 10 IPCC AR-4 generalized circulation models (GCMs; ensemble mean with SE) for each of four ice seasons and annually; (lower histograms) the corresponding within-season percentage change in optimal habitat area relative to the first (1985–1995) decadal period.

accommodate differences in habitat selection caused by regional differences in sea ice composition and dynamics (Wadhams 2000); and (3) the tracking data were disproportionately distributed (Fig. 4).

We observed differences in RSF performance among subpopulations (Table 7). Model performances tended to be less robust in subpopulations spanning the broad Eurasian continental shelf, and more robust in the Barents Sea and the subpopulations bordering North America. Nevertheless, in all cases, the top 50% of the RSF-valued habitats were occupied by a substantive majority ($\geq$70%) of the polar bear locations. This demonstrated that, despite inter-regional differences in performance, the RSF models were robust throughout the polar basin.

Applicability of retrospective RSFs to 21st-century sea ice projections

We structured our RSF analysis seasonally, based on quantifiable patterns in the annual cycle of sea ice growth and melt, because sea ice in the Arctic Ocean undergoes significant changes in extent and composition each year. Yet despite the pronounced differences in habitat conditions and dynamics between seasons, each

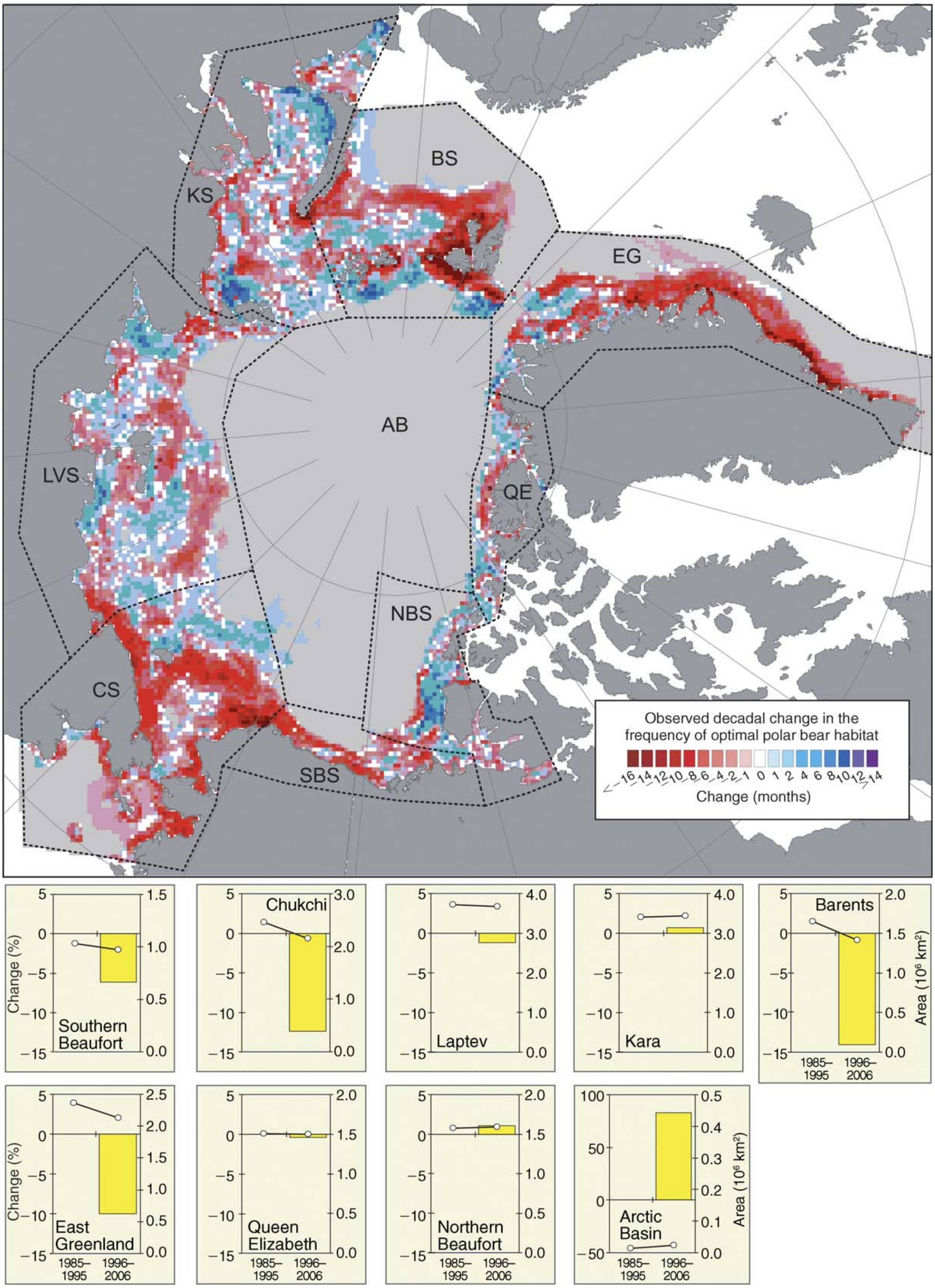

FIG. 12. Observed changes in the spatial distribution and integrated annual area of optimal polar bear habitat. The base map shows the cumulative number of months per decadal period where optimal polar bear habitat was either lost (red) or gained (blue) from 1985 through 1995 to 1996 through 2006. Offshore gray shading denotes areas where optimal habitat was absent in both periods.

of the best seasonal RSFs had remarkably similar covariate structure. These covariates may be considered important to polar bears throughout the year. However, magnitudes of covariate parameter estimates did differ seasonally, indicating that the response by polar bears to the covariates varied during the course of the annual sea ice cycle.

Consistent RSF performance between two decades of observational data suggests the models are robust for evaluating future sea ice conditions. When we applied the RSFs (which were derived with 1985–1995 data) to an independent set of observed sea ice and polar bear location data from 1996 to 2006, more than 80% of polar bear locations from the 1996–2006 period occurred in the top 20% of RSF-valued habitats (Fig. 7). High RSF performance persisted in the recent decade, despite large environmental changes that included many of the lowest summer ice extents on record. Hence, consistent performance of the RSFs during a time of markedly different sea ice conditions supports the validity of using these retrospective models to evaluate how polar bear habitats may change during the 21st century.

Variability among GCMs

The specific greenhouse gas emission scenario that is used to force a GCM is a key determinant of its projection outcome. The IPCC SRES 21st century forcing scenarios were designed to capture a range of political and societal responses to the economic and environmental concerns of global warming. Three SRES forcing scenarios, the B1, A1B, and A2, respectively, attain atmospheric CO_2 concentration levels of 546, 717, and 856 ppm by the year 2100. Zhang and Walsh (2006) used these scenarios to calculate the decrease in ensemble-mean summer-ice minimum area for 1979–1999 and 2080–2100 and obtained reductions of 45.8%, 59.7%, and 65.0% of sea ice in the B1, A1B, and A2 scenarios, respectively.

We focused our analyses on the A1B middle range "business as usual" scenario. Our cursory comparisons with CCSM3 ice projections based on the SRES-B1 scenario (reduced carbon forcing; Figs. 9 and 10 and Table 8) showed a slower rate of sea ice loss (Fig. 9a) and hence a slower loss of optimal polar bear habitat (Fig. 10, Table 8). The converse should hold for a more aggressive assumption of greenhouse gas loading (e.g., SRES-A2). But even the relatively optimistic B1 scenario, when applied by CCSM3, projected as much as a 70% loss of optimal habitat in the Barents Sea by the end of the century (Fig. 10).

Close inspection of the CCSM3 ice projections shows that trajectories of the A1B and B1 forcing scenarios are very similar until about 2030, after which they begin an obvious departure (Fig. 9a). Differences between the A1B and B1 scenarios (for the CCSM3 model) in timing and relative magnitude of projected sea ice extent are very similar to the inverse of their imposed CO_2 loadings (data *available online*).[18]

Twenty-first century habitat distribution and trends

Projected losses of polar bear habitat during the 21st century varied among GCMs and forcing scenarios. This scatter reflects many interacting GCM-specific factors (DeWeaver 2007, Overland and Wang 2007) including the initial (late 20th century) ice thickness, aspects of the modeled ocean circulation, the treatment of surface albedo (the fraction of shortwave solar energy reflected back into space) and the amount and radiative properties of clouds. In general, declines in optimal sea ice habitat accelerated from early in the 21st century until about 2075. Rates of habitat loss declined after 2075 because several models had already reached near ice-free summers by this time (Fig. 9).

The observed habitat changes from 1985 through 1995 to 1996 through 2006 established a trajectory that was generally perpetuated by the 21st-century sea ice projections. In many cases, the observed rates of habitat change exceeded those of the GCMs, revealing a "faster than forecast" signature (Stroeve et al. 2007) in polar bear habitat loss as well as sea ice loss. This is likely because that as a group, the IPCC-AR4 models tend to underestimate the impacts of greenhouse gas loading (Stroeve et al. 2007). The "faster than forecast" effect is clearly evident for the changes in summer ice extent, and particularly so for summer 2007 when new record minima in ice extent and area were reached (Maslanik et al. 2007*b*).

Rates and trends in observed habitat changes between 1985–1995 and 1996–2006 were not identical throughout the circumpolar Arctic basin. The observed record revealed that the greatest losses of optimal polar bear habitat occurred in the peripheral seas of the Arctic Ocean while interior regions (i.e., the Arctic Basin and Queen Elizabeth) remained relatively stable (Fig. 12). In particular, the observational data showed the largest decline of optimal habitat in the Chukchi and Barents seas, while only modest declines characterize the Kara and Laptev seas. Differences among polar bear subpopulations distributed around the edges of the polar basin likely stem from differences in oceanography: both the Chukchi and Barents seas are more directly influenced by the warmer waters of the Pacific and Atlantic oceans, respectively (Macdonald and Bewers 1996, Woodgate et al. 2006), as well as regional effects of atmospheric circulation (Rigor et al. 2002, Maslanik et al. 2007*a*). The magnitude of predicted habitat loss in the peripheral regions of the Arctic Ocean was not offset by modest increases in the interior Arctic Ocean; hence,

←
Insets show the mean annual (12 month) cumulative area of optimal habitat (right *y*-axis, line plot) for the two 11-year periods (*x*-axis), and their associated percentage change in area (left *y*-axis, histograms) relative to the first period (1985–1995). Place names use the same letter codes as defined in Fig. 1.

---

[18] ⟨http://www.cccma.ec.gc.ca/data/cgcm3/cgcm3_forcing.shtml⟩

TABLE 8. Mean rates of change (percentage per decade) in the annual cumulative area of optimal polar bear habitat based on sea ice projections by 10 IPCC AR-4 general circulation models (GCM) and their ensemble mean.

Location, time period	Optimal habitat change (%)†	Annual change in optimal habitat (km^2)‡	General circulation models (GCM)					
			Ensemble	ccsm3 A1B	ccsm3 B1	cgcm3	cnrm	gfdl
Full study area	−5.0**	1 464 000						
2001–2099			−4.0**	−4.9**	−2.7**	−2.4**	−3.5**	−2.4**
2001–2050			−3.7**	−6.2**	−4.0**	−2.6**	−3.2**	−1.4**
2050–2075			−6.1**	−4.7**	−3.3**	0.8	−4.3**	−5.8**
2075–2099			−3.1**	−2.7**	−1.0*	−1.7	−4.1**	−0.7
Convergent	−4.0**	453 000						
2001–2099			−3.0**	−3.4**	−1.5**	−1.7**	−2.6**	−1.6**
2001–2050			−2.7**	−3.8**	−2.4**	−1.5†	−2.8**	−1.0*
2050–2075			−4.2**	−3.7**	−2.7**	−0.2	−2.5†	−4.2**
2075–2099			−2.6**	−2.3**	0.2	2.6	−4.4*	−0.8
Divergent	−5.5**	1 011 000						
2001–2099			−4.3**	−5.8**	−3.4**	−2.7**	−3.7**	−2.7**
2001–2050			−4.2**	−7.4**	−4.9**	−3.0**	−3.4**	−1.5**
2050–2075			−7.0**	−5.4**	−3.6**	1.2	−4.8**	−6.4**
2075–2099			−3.4**	−2.9**	−1.7*	−3.5†	−4.0**	−0.7
Queen Elizabeth	−1.9	127 000						
2001–2099			−0.9**	−2.0**	−0.4**	1.3**	−1.7**	0.0
2001–2050			0.7**	−0.8**	−0.4	1.7*	−0.6	1.7**
2050–2075			−2.3**	−3.4*	−1.6	0.3	−4.1*	−0.5
2075–2099			−2.2**	−3.4*	0.2	6.1*	−5.9*	−0.6
East Greenland	−7.7**	193 000						
2001–2099			−4.3**	−4.2**	−2.4**	−2.2**	−2.7**	−2.3**
2001–2050			−4.8**	−6.0**	−4.3**	−1.8†	−2.7**	−2.8**
2050–2075			−5.1**	−4.5**	−1.6†	−2.6	−1.5	−5.1*
2075–2099			−2.9†	−1.3	0.0	0.7	−4.7†	−0.3
Barents Sea	−10.7**	131 000						
2001–2099			−6.5**	−11.5**	−8.0**	−2.7**	−5.8**	−4.5**
2001–2050			−5.9**	−14.2**	−11.3**	−3.8**	−3.8**	−2.4**
2050–2075			−13.1**	−29.8**	−15.6**	4.0	−2.9	−9.5*
2075–2099			−0.3	−21.1**	−9.6*	−5.6†	−9.2**	7.0
Kara Sea	−5.1*	291 000						
2001–2099			−4.2**	−5.1**	−3.3**	−1.5**	−3.0**	−2.6**
2001–2050			−3.3**	−7.3**	−4.5**	−1.2	−2.1**	−1.1
2050–2075			−6.7**	−6.6**	−3.3*	4.4†	0.1	−4.2*
2075–2099			−2.6†	−2.6	−1.0	−3.6	−3.1	−0.2
Laptev Sea	−1.9	309 000						
2001–2099			−2.4**	−4.0**	−2.2**	−1.0**	−2.3**	−1.3**
2001–2050			−2.3**	−4.8**	−2.4**	−1.5*	−0.8	−0.6
2050–2075			−4.1**	−2.6**	−0.4	0.5	−7.9**	−3.5
2075–2099			−2.7*	−2.4†	−2.8†	0.2	−2.4	−1.4
Chukchi Sea	−8.0**	196 000						
2001–2099			−5.3**	−6.4**	−3.4**	−5.4**	−5.1**	−3.3**
2001–2050			−6.1**	−8.1**	−5.7**	−6.0**	−7.4**	−2.2**
2050–2075			−7.8**	−4.2	−2.7	−3.5	−8.6**	−9.5**
2075–2099			−7.5**	−2.0	−0.7	−8.7†	−5.1	−3.8
Southern Beaufort Sea	−4.8	84 000						
2001–2099			−5.2**	−5.3**	−2.7**	−5.0**	−4.5**	−2.8**
2001–2050			−5.9**	−6.6**	−3.8**	−4.0†	−6.6**	−2.3*
2050–2075			−8.8**	−4.0†	−7.3**	0.2	−3.9	−12.0**
2075–2099			−4.2*	−3.6	1.6	−3.3	−3.8	−1.8
Northern Beaufort Sea	−0.2	132 000						
2001–2099			−3.5**	−3.5**	−1.4**	−3.7**	−3.5**	−2.2**
2001–2050			−3.3**	−3.2**	−1.4**	−3.7*	−5.2**	−1.1*
2050–2075			−5.4**	−2.5†	−5.1**	2.1	−1.4	−6.9**
2075–2099			−2.8*	−2.6*	0.7	0.4	−2.0	−1.3

Table 8. Extended.

General circulation models (GCM)					
giss	hadgem	ipsl	miroc	miub	mpi
−1.5**	−5.3**	−3.1**	−5.7**	−2.9**	−6.7**
−3.3**	−4.3**	−4.7**	−3.0**	−1.7**	−6.6**
0.2	−9.4**	−4.3*	−10.8**	−4.9**	−16.8**
1.9	−10.8**	4.3†	−11.5**	−5.1*	−2.6
−0.6*	−3.4**	−2.3**	−5.0**	−1.5**	−5.9**
−1.0	−2.5**	−3.0**	−3.0**	−0.2	−5.8**
−1.2	−7.5**	3.5†	−10.3**	−3.4	−10.8**
1.8	−10.6**	−4.5†	−6.3**	1.5	−2.9
−1.8**	−6.1**	−3.5**	−5.9**	−3.5**	−7.1**
−4.0**	−5.0**	−5.5**	−3.0**	−2.3**	−7.0**
0.7	−10.4**	−8.2*	−11.0**	−5.6*	−19.6**
1.9	−11.0**	10.3**	−13.5**	−8.0**	−2.4
1.2**	−1.5**	0.7**	−3.3**	0.5*	−2.9**
2.6**	0.1	1.1*	0.7*	2.5**	−1.0†
−1.0	−3.9*	5.6*	−10.4**	−2.3	−3.3
−0.8	−7.0**	−1.8	−5.3*	−0.2	−3.9
−0.9	−5.2**	−3.7**	−6.6**	−2.3**	−8.1**
−2.8*	−4.5**	−4.0**	−6.4**	−2.9*	−9.3**
2.1	−12.2**	2.5	−9.9**	1.3	−15.0**
9.4	−14.0**	−6.8	−10.4**	9.0*	−5.4
0.3	−11.5**	−3.8**	−10.1**	−5.5**	−10.9**
−4.5**	−11.1**	−3.2*	−2.9**	−1.1	−14.3**
−1.9	−30.6**	−17.3**	−31.0**	−10.1**	−34.2**
7.1*	−17.5	20.7*	−42.7**	−9.1**	51.1
−1.2**	−6.8**	−3.0**	−6.8**	−4.3**	−8.8**
−1.9†	−5.1**	−2.6	−2.0*	−2.1†	−9.4**
4.9	−13.9**	−15.5**	−15.9**	−7.3**	−20.8**
1.7	−13.0*	15.8†	−18.7**	−9.3*	6.2
−1.3**	−4.1**	−1.9**	−2.3**	−2.2**	−3.9**
−3.1**	−2.6**	−6.0**	−0.8†	−1.9†	−1.3
0.3	−8.9**	−0.2	−1.9	−2.1	−11.9**
−0.8	−6.6**	5.9†	−4.7†	−11.1**	−1.7
−4.2**	−5.5**	−6.0**	−6.7**	−2.2**	−6.8**
−8.1**	−4.1**	−11.6**	−6.5**	−3.8**	−6.0**
−1.8	−5.6*	20.3*	−6.2	−1.8	−23.0**
3.8	−15.4**	−5.6	−19.2**	0.0	−14.4**
−4.4**	−4.5**	−9.8**	−4.7**	−3.7**	−7.9**
−6.5**	−5.3**	−15.1**	−4.0*	−3.0†	−8.3**
−7.4	−7.4	8.1	−9.6	−10.8**	−24.0**
0.3	−9.9*	−15.2	−8.5	−5.3	5.4
−2.3**	−3.0**	−3.7**	−4.8**	−2.4**	−5.5**
−3.2*	−2.7**	−6.2**	−2.7†	−0.5	−4.7**
−3.8	−6.0	1.3	−10.6†	−8.0	−14.5**
−0.5	−10.5**	−6.7	−3.0	−1.2	1.1

there was a net loss in optimal polar bear habitat during the observational period, 1985–2006.

Similar spatial patterns of habitat loss were projected for the mid-21st century (Fig. 13). Large habitat losses were also projected, however, for the Kara and Laptev seas, rendering those subpopulations consistent with the observed and projected declines in other Divergent ecoregion subpopulations. In the Northern Beaufort Sea subpopulation, little net change in optimal habitat was projected until mid-century (Fig. 10b), after which net losses commenced in all but the most northerly sector (Fig. 13). Also consistent with observations, optimal habitat was likely to be sustained in the Arctic Basin and Queen Elizabeth subpopulations until about 2050, with changes thereafter remaining small.

By the end of the 21st century, the annual average annually integrated area of optimal polar bear habitat was projected to decline from its observed value of 1.5 million km^2 in 1985–1995 to 1.0 million km^2 (–32% change, Fig. 11). This annual change combined ~6 winter months (Fig. 5), in which there was little change in optimal habitat, with more dramatic changes during the spring (–55%), summer (–68%), and autumn (–27%, Fig. 11). In both the observational period and in the 21st-century projections, the greatest reductions in optimal habitat occur during summer. By the mid-21st century, most peripheral seas have very little optimal polar bear habitat remaining during summer. The combination of spatial and temporal loss of optimal habitat by the end of the 21st century results in large reductions in the availability of the habitats polar bears prefer.

In contrast, optimal polar bear habitat returns in winter throughout most of its former range. An exception to this, however, is the Barents Sea, where high-value RSF pixels were largely absent even during winter in the later part of the 21st century (Fig. 8). Collectively, spring and summer represent about four months of the annual cycle (Fig. 5), so the loss of optimal habitat during spring and summer has temporal, as well as spatial, significance.

While projected trends in habitat were similar to changes in sea ice, sea ice alone did not fully explain the distribution of polar bear habitat because ocean depth was a strong covariate in all seasons. Persistent sea ice in the Arctic Basin subpopulation did not translate into large areas of optimal habitat because the region is predominantly deep water. In contrast, the nearby Queen Elizabeth subpopulation, which had ice characteristics similar to the Arctic Basin, also encompassed shallow continental shelf waters. This translated into an increase of high-value RSF habitat by the mid-21st century (Fig. 13).

Ecological interpretation of the RSF covariates

Polar bears in the Pelagic ecoregions selected ice concentrations near 80% in spring, 65% during summer, 60% in autumn, and 95% in winter. In the Canadian

TABLE 8. Continued.

Location, time period	Optimal habitat change (%)†	Annual change in optimal habitat (km^2)‡	General circulation models (GCM)					
			Ensemble	ccsm3 A1B	ccsm3 B1	cgcm3	cnrm	gfdl
Arctic Basin	33.9*	2000						
2001–2099			1.6*	−2.2**	1.1*	13.3**	−4.1**	3.7
2001–2050			12.9**	3.3*	3.3**	3.8	−0.5	19.2*
2050–2075			−0.9	−9.3**	2.8	21.8†	−22.0*	−0.9
2075–2099			−3.8	−9.0*	−7.5*	15.5	10.2	−16.8

Notes: Rates of change (percentage per decade) were calculated from estimates of slope (total area per year) based on linear regression analysis with the annual cumulative area of optimal habitat as the dependent variable and year as the independent variable. All GCMs were forced with the IPCC SRES-A1B scenario, and results for CCSM3 under the SRES-B1 scenario are additionally shown. Statistical significance of estimates of percentage change: †$P < 0.10$; *$P < 0.05$; **$P < 0.01$.

† For comparison, the rate of optimal habitat change based on satellite observations of sea ice during 1979–2006 is shown.

‡ To help gauge relative sizes of areas of optimal sea ice in each IUCN during 1979–2006, the mean annual cumulative area (km^2) of optimal habitat during 1979–2006 is shown.

archipelago, Ferguson et al. (2000) found that polar bears were highly selective for habitats with >90% sea ice throughout the year. Ferguson et al. (2000) also observed that even within the Seasonal Ice ecoregion of Baffin Bay, polar bears selected sea ice concentrations ≥95% during autumn through spring. Only during summer in Baffin Bay (Seasonal Ice ecoregion) did polar bears demonstrate selection for ice concentrations <70% (Ferguson et al. 2000). Durner et al. (2004) found that polar bears in the Beaufort Sea selected sea ice near 100% concentration in spring and 70–80% in autumn. The selection for moderate sea ice concentration that we document during spring through autumn throughout the Pelagic ecoregion was similar to that reported by Mauritzen et al. (2003*a*) for the Barents Sea, and by Arthur et al. (1996) and Durner et al. (2006) for the Chukchi Sea. These studies suggest that patterns of spatial use of sea ice by polar bears vary among the ecoregions defined by Amstrup et al. (2007) and that it is appropriate to define ecoregion-specific habitat models.

The seasonal variation in selection of ice concentration may be a response by polar bears to balance foraging and refuge requirements (Mauritzen et al. 2003*a*); bears position themselves in the most optimal habitat for hunting seals but at the same time select sea ice that will provide safety from ocean storms or becoming separated from the main ice pack. This may explain why polar bears used areas with relatively high ice concentration in close proximity to areas with very low (15%) ice concentrations during spring through autumn. In a study of polar bear spatial patterns for the Barents Sea, Mauritzen et al. (2003*a*) observed similar behavior by bears to avoid low ice concentrations near the open ocean.

Similar to total sea ice concentration, response to the 15% ice concentration threshold varied seasonally. As the spring melt began, polar bears continued to use areas with relatively high ice concentrations, but they also showed the lowest degree of selection for the 15% ice threshold, possibly to avoid the open ocean near the edge of the retreating pack. The opposite occurred during autumn, which, as a season of ice extent similar to spring, polar bears showed greater selection for the 15% ice threshold than at any other time of year. Different response to the 15% threshold in spring and autumn suggests an ability of bears to anticipate seasonal changes in sea ice (Ferguson et al. 2000). It is likely that polar bears in the pelagic ecoregions position themselves near the rapidly increasing autumn ice edge to expedite their return to hunting habitats over shallow continental shelf waters and with little risk of being marooned, away from the main pack. The ability of polar bears to learn energetically efficient responses to changing ice concentrations has also been demonstrated in Western Hudson Bay. Stirling et al. (1999) demonstrated that as the ice along the coast melted in spring, bears came ashore ~2.5 weeks after the ice cover was reduced to 50%. In this circumstance, it would be safe for a polar bear to remain on the ice as it continued to break up, as long as it was still energetically efficient to continue to hunt seals, because they have a relatively short swim to land where they then fast for several months until Hudson Bay refreezes.

Distance to land, rather than distance to the 15% ice concentration threshold, entered the best winter RSF, but these two covariates were highly correlated in winter and can be considered functionally equivalent. Although polar bears selected high ice concentrations during winter, selection for sea ice near shore may be an attempt to maintain close proximity to the broken sea ice in nearshore flaw zones and polynyas (open areas of water surrounded by sea ice) where prey may be most available (Stirling et al. 1993, Stirling 1997).

Polar bears throughout the pelagic ecoregions selected ice over relatively shallow seas throughout the year. The response that we observed was similar to that of Durner et al. (2004) who reported that polar bears in the Beaufort Sea selected habitats over the shallowest waters available. Polar bear distribution relative to ocean depth appears consistent with expected prey distribution. Polar

Table 8. Extended. Continued.

General circulation models (GCM)					
giss	hadgem	ipsl	miroc	miub	mpi
2.7*	12.1**	10.8**	−3.5*	−2.9**	0.4
6.8*	33.4**	12.5*	29.8**	13.7**	15.9**
8.9	9.1	8.0	−15.0	−6.4	4.1
1.3	−20.6**	47.3*	−15.7	−10.0	−9.4

bears within the study area are mostly dependent on young of the year ringed seals (Stirling and Øritsland 1995), whose distribution is primarily in broken ice over shallow waters (Born et al. 2004). Polar bears also prey on bearded seals (Derocher et al. 2002), whose benthic feeding habitats (Burns 1981) generally limit their distribution to open ice habitats over the continental shelves (Gjertz et al. 2000). Therefore, the response of polar bears to bathymetry, as it appears in the RSFs, is consistent with expected prey distributions.

The impacts of projected changes in sea ice habitat on polar bears are not likely to be proportional to the length of season. During spring and early summer, polar bears require a substrate of nearshore sea ice to access recently weaned and naive seals (Stirling and Archibald 1977, Smith 1980). In the southern Beaufort Sea, much of the annual gain in body mass occurs during autumn when polar bears move from the deep-water pack ice to newly formed ice in shallow water regions (Durner and Amstrup 1996) where seal densities are higher. Therefore, the consequences of projected high losses of spring through autumn sea ice habitat may be amplified by reducing or eliminating hunting opportunities during the most significant feeding seasons to polar bears inhabiting the Arctic Ocean.

Consequences of habitat change on polar bear distributions

Polar bears show fidelity to geographic regions (Amstrup et al. 2000) such that populations may be defined by the movements of individuals (Bethke et al. 1996, Taylor et al. 2001, Mauritzen et al. 2002, Amstrup et al. 2004). It is reasonable, therefore, to assume that individuals would attempt to return to their region of origin even when their habitat undergoes extreme seasonal redistribution. We projected large differences in amount and distribution of summer and winter optimal polar bear habitat for the 21st century. This evokes questions regarding the movements and distribution of polar bears as they contend with what may be extreme minimum ice seasons in the future. We suggest that polar bears living in ecoregions with dynamic pack ice will be required to "make decisions" in response to increasing seasonal amplitudes in sea ice extent. They must either follow the sea ice to higher latitudes where the ice may persist (but possibly over less productive waters) or choose to remain nearby their traditional foraging ranges by summering on land and fasting, as bears already do each year in the seasonal ice region. Bears that move north in the summer with the retreating sea ice then must decide if returning to traditional nearshore winter areas is a better option than simply remaining in an area where sea ice is relatively persistent throughout the year. Ultimately, the relative rates of survival, reproduction, and recruitment of bears that choose different options will determine which strategy is most successful and favored by natural selection.

Polar bears in the Divergent ecoregion that follow the retreating summer pack ice will enter regions already occupied by other populations of polar bears. The carrying capacity of polar bear habitat is unknown, but the relatively small world population is presently distributed over a very large geographic area. While density-dependent responses are not well understood for polar bears (Derocher and Taylor 1994), it is likely that as the world population of polar bears is forced into smaller areas of habitat, individual reproductive fitness will decline because of density-dependent effects (McLoughlin et al. 2006).

Either following the ice or summering on land likely imposes different energetic costs (Mauritzen et al. 2003*b*). Available evidence suggests that polar bears are largely food deprived while on land (Ramsay and Hobson 1991). Therefore, polar bears that summer on land must gain sufficient mass prior to going ashore to survive an extended fast. While summering on land has been an effective strategy for some populations of polar bears living in prey-rich environments, such as Hudson Bay and Baffin Bay, recent evidence suggests there are limitations, even in those regions, to the amount of time that polar bears can remain on land and still maintain a viable population (Stirling and Parkinson 2006, Regehr et al. 2007). Obtaining sufficient body mass to survive an extended summer fast may be even more problematic for polar bears that typically live over the shelf regions of the Arctic Ocean. As the amount of habitat decreases during spring and autumn, polar bears will be increasingly displaced from the narrow shelf and from most seal prey. This suggests that an extended summer fast may not be possible for some polar bear subpopulations in the Arctic Ocean, if their ability to accumulate sufficient mass gain during the intervening period becomes too severely compromised. Reduced body stores could compromise reproductive success, and therefore recruitment, by causing bears to forgo maternal denning or reducing the survival of neonates (Atkinson and Ramsay 1995).

Assuming that the RSF predictions of polar bear habitat are robust, by the mid-21st century most bears choosing to follow the retreating spring sea ice will occupy coastal zones in the Queen Elizabeth subpopulation and the most northern reaches of the Northern Beaufort subpopulation during summer. Distances traveled between summer and winter ranges will be

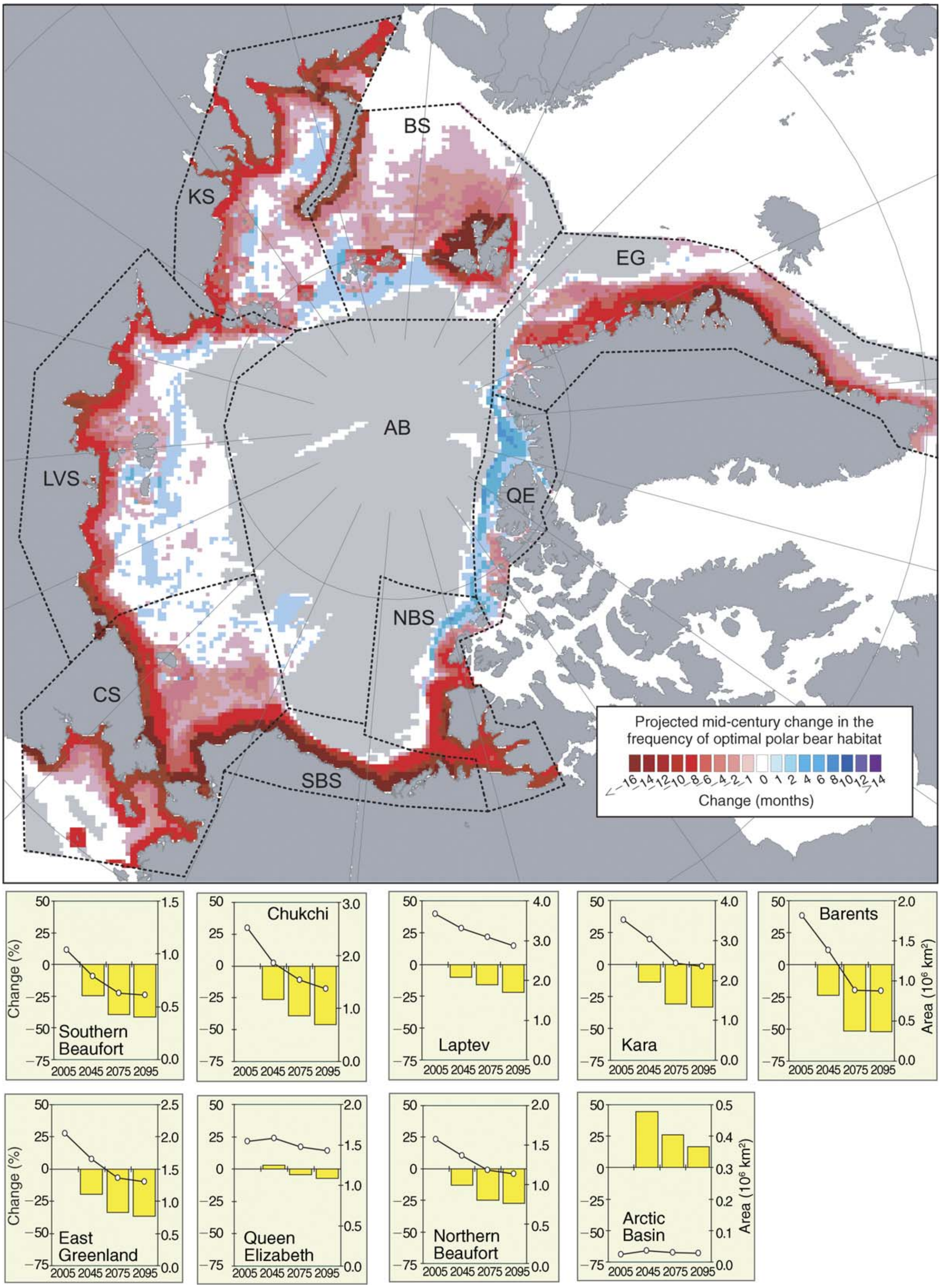

FIG. 13. Projected changes (based on 10 IPCC AR-4 general circulation models [GCMs] run with the SRES-A1B forcing scenario) in the spatial distribution and integrated annual area of optimal polar bear habitat. The base map shows the cumulative number of months per decade where optimal polar bear habitat was either lost (red) or gained (blue) from 2001 through 2010 to

greatest for those bears that winter along the Eurasia coast and least for bears that winter near the Canadian coast. The autumn return of polar bears to nearshore sea ice habitat along the northern Chukota coast has been observed to occur two to three weeks later than what was observed in the 1980s, apparently because of the greater summer ice retreat in the Chukchi and East Siberian seas since 1995 (S. E. Belikov, *unpublished data*). Polar bears, however, are capable of sustained movement rates >4 km/hr (Amstrup et al. 2000) and may travel an mean of >5000 km/year in response to seasonal extremes in sea ice distribution (Garner et al. 1990).

Extensive movements to and from remnant summer habitats and traditional winter ranges, however, will likely impose greater energetic demands on some age/sex classes compared to others (Derocher and Taylor 1994). Polar bears have demonstrated fidelity to geographic regions for maternal denning (Ramsay and Stirling 1990, Amstrup and Gardner 1994). For pregnant polar bears, returning to traditional terrestrial denning locales could become energetically prohibitive if they chose to summer on high-latitude ice cover. Pregnant polar bears must have adequate lipid reserves prior to denning to maximize survival of their neonates (Atkinson and Ramsay 1995). Lactation imposes additional energy demands on females with young (Thiemann et al. 2005). Mobility of females with first-year young is less than that of other reproductive classes (Ferguson et al. 1997, Amstrup et al. 2000), and they may avoid active drift ice (Mauritzen et al. 2003*b*). Therefore, long-distance movements to and from the Divergent ecoregion may place the greatest demands on pregnant bears and bears with dependent young, and may ultimately impact reproductive success and population recruitment.

Conclusions

We developed RSF models of polar bear habitat utilization using empirical data of polar bear movements and sea ice conditions during 1985–1995 in the Arctic Ocean and peripheral seas of the polar basin. We then extrapolated the RSF models using (1) observed sea ice conditions during 1996–2006 and (2) projected sea ice conditions during the 21st century, to assess both recent and future changes in the extent and distribution of polar bear habitats in the polar basin. The 21st-century sea ice projections were extracted from 10 IPCC AR-4 general circulation models which had 20th-century ice simulations that were reasonably concordant with the observational sea ice record of minimum summer ice extent. The following points summarize the main results of this study:

1) Polar bears preferred habitats that were over shallower water (continental shelf), partially covered by sea ice, and closer to land during winter. Projected loss of sea ice typically translates to loss of preferred polar bear habitat because the spatial pattern of melt is generally from the periphery of the ice pack (shelf waters) poleward.

2) Projected losses in ice extent were pronounced in spring and summer, but the ice cover was largely restored each winter, so amplitude of the annual oscillation in sea ice extent increased. Hence, expected changes in polar bear habitat extent will be strongly seasonal, with dramatic losses in spring and summer and modest to negligible losses in winter.

3) Observed decadal changes from 1985 through 1995 to 1996 through 2006 showed pronounced losses of polar bear habitat during the spring and summer in the Southern Beaufort, Chukchi, Barents, and East Greenland seas. Projected habitat losses during the 21st century were spatially and seasonally consistent with observed trajectories, with the addition of pronounced losses in the nearshore regions of the Laptev and Kara seas.

4) By the end of the 21st century, only modest net annual habitat losses were projected for areas north of the Canadian archipelago and Greenland, suggesting that these regions will have the greatest likelihood of sustaining viable, albeit smaller, polar bear populations.

5) An increased seasonal amplitude in ice extent will require polar bears inhabiting Alaska and Eurasia to either migrate long distances to remain on the ice or spend summers stranded on land. Either scenario presents energetic challenges that could jeopardize long-term residency of the Divergent ecoregion polar bear subpopulations.

6) Observed rates of habitat loss during the past two decades defined a trajectory that has greater negative slope than that simulated by most GCMs. As such, habitat losses through the 21st century based on multi-model GCM means may be conservative.

Acknowledgments

Funding for this analysis was provided by the U.S. Geological Survey and the U.S. Fish and Wildlife Service. Tagging studies that provided polar bear location data from the Chukchi and Beaufort seas in the United States were supported, in part, by B. P. Exploration–Alaska, ConocoPhillips–Alaska, the U.S. Minerals Management Service, and the North Slope Borough Department of Wildlife Management. We thank Dennis Andriashek, Steve Arthur, Andrei Boltunov, Per Espen Fjeld, Anthony Fischbach, Craig Gardner, Michael Lockhart, Nick Lunn, Eric Regehr, Kristin Simac, Jørn Thomassen, and Geoff York for assistance in the field. We gratefully acknowledge the accomplishments of Gerald Garner (USGS, Alaska

---

←

2041 through 2050. Offshore gray shading denotes areas where optimal habitat was absent in both periods. Insets show the mean annual (12 month) cumulative area of optimal habitat (right *y*-axis, line plot) for four 10-year periods in the 21st century (*x*-axis midpoints), and their associated percentage change in area (left *y*-axis, histograms) relative to the first decade (2001–2010). Place names use the same letter codes as defined in Fig. 1.

Science Center) (deceased) who, through a cooperative effort with the All-Russian Research Institute for Nature Protection, deployed many of the satellite-radio collars in the Russian Chukchi Sea and along the Siberian coast. The Alfred Wegener Institute of Marine Research (Bremerhaven, Germany) is thanked for logistical support during the East Greenland studies. We thank Bryan Manly, Karen Oakley, Martyn Obbard, and an anonymous reviewer for constructive suggestions to earlier versions of this manuscript. We acknowledge the many international global climate modeling groups for making their simulations available to the scientific community, the Program for Climate Model Diagnosis and Intercomparison (PCMDI) for collecting and archiving the CMIP3 model output, and the WCRP's Working Group on Coupled Modelling (WGCM) for organizing the model data analysis activity. The WCRP CMIP3 multi-model data set is supported by the Office of Science, U.S. Department of Energy. Eric DeWeaver is supported through DOE grant DE-FG02-03ER63604. We acknowledge the National Science Foundation for support of several of our collaborators. Any use of trade, product, or firm names is for descriptive purposes only and does not imply endorsement by the U.S. Government.

LITERATURE CITED

Aars, J., N. J. Lunn, and A. E. Derocher. 2006. Polar bears. Occasional paper 32. Proceedings of the 14th Working Meeting of the IUCN/SSC Polar Bear Specialist Group, June 20–24 2005, Seattle, Washington, USA.

Amstrup, S. C. 2003. Polar bear, *Ursus maritimus*. Pages 587–610 *in* G. A. Feldhamer, B. C. Thompson, and J. A. Chapman, editors. Wild mammals of North America: biology, management, and conservation. Second edition. Johns Hopkins University Press, Baltimore, Maryland, USA.

Amstrup, S. C., G. M. Durner, I. Stirling, N. Lunn, and F. Messier. 2000. Movements and distribution of polar bears in the Beaufort Sea. Canadian Journal of Zoology 78: 948–966.

Amstrup, S. C., and C. Gardner. 1994. Polar bear maternity denning in the Beaufort Sea. Journal of Wildlife Management 58:1–10.

Amstrup, S. C., B. G. Marcot, and D. C. Douglas. 2007. Forecasting the rangewide status of polar bears at selected times in the 21st century. Administrative Report. U.S. Geological Survey, Alaska Science Center, Anchorage, Alaska, USA.

Amstrup, S. C., T. L. McDonald, and G. M. Durner. 2004. Using satellite radiotelemetry data to delineate and manage wildlife populations. Wildlife Society Bulletin 32:661–679.

Amstrup, S. C., I. Stirling, T. S. Smith, C. Perham, and G. W. Thiemann. 2006. Intraspecific predation and cannibalism among polar bears in the southern Beaufort Sea. Polar Biology 29:997–1002.

Arthur, S. M., B. F. J. Manly, L. L. McDonald, and G. W. Garner. 1996. Assessing habitat selection when availability changes. Ecology 77:215–227.

Atkinson, S. N., and M. A. Ramsay. 1995. Effects of prolonged fasting of the body composition and reproductive success of female polar bears (*Ursus maritimus*). Functional Ecology 9: 559–567.

Belchansky, G. I., D. C. Douglas, and N. G. Platonov. 2004. Duration of the Arctic sea ice melt season: regional and interannual variability, 1979–2001. Journal of Climate 17: 67–80.

Belchansky, G. I., D. C. Douglas, and N. G. Platonov. 2005. Spatial and temporal variations in the age structure of Arctic sea ice. Geophysical Research Letters 32:L18504.

Bethke, R., M. Taylor, S. Amstrup, and F. Messier. 1996. Population delineation of polar bears using satellite collar data. Ecological Applications 6:311–317.

Bodmer, R. E., J. F. Eisenburg, and K. H. Redford. 1997. Hunting and the likelihood of extinction of Amazonian mammals. Conservation Biology 11:460–466.

Born, E. W., J. Teilmann, M. Acquarone, and F. F. Riget. 2004. Habitat use of ringed seals (*Phoca hispida*) in the North Water area (North Baffin Bay). Arctic 57:129–142.

Burnham, K. P., and D. R. Anderson. 2002. Model selection and multimodel inference. Second edition. Springer-Verlag, New York, New York, USA.

Burns, J. J. 1981. Bearded seal *Erignathus barbatus* Erxleben, 1777. Pages 145–170 *in* S. H. Ridgeway and R. J. Harrison, editors. Handbook of marine mammals. II: Seals. Academic Press, London, UK.

CAPE Last Interglacial Project Members. 2006. Last Interglacial arctic warmth confirms polar amplification of climate change. Quaternary Science Reviews 25:1383–1400.

Cavalieri, D., C. Parkinson, P. Gloersen, and H. J. Zwally. 2006. Sea ice concentrations from Nimbus-7 SMMR and DMSP SSM/I passive microwave data. National Snow and Ice Data Center, Boulder, Colorado, USA.

Comiso, J. C. 2006. Abrupt decline in the Arctic winter sea ice cover. Geophysical Research Letters 33:L18504.

Conover, W. J. 1980. Practical nonparametric statistics. Second edition. John Wiley and Sons, New York, New York, USA.

Cooper, A. B., and J. J. Millspaugh. 1999. Application of discrete choice models to wildlife resource selection studies. Ecology 80:566–575.

Davies, K. F., C. R. Margules, and J. F. Lawrence. 2004. Synergistic effect puts rare, specialized species at greater risk of extinction. Ecology 85:265–271.

Derocher, A. E., N. J. Lunn, and I. Stirling. 2004. Polar bears in a warming climate. Integrative and Comparative Biology 44: 163–176.

Derocher, A. E., and I. Stirling. 1990. Distribution of polar bears (*Ursus maritimus*) during the ice-free period in western Hudson Bay. Canadian Journal of Zoology 68:1395–1403.

Derocher, A. E., and M. Taylor. 1994. Density-dependent population regulation of polar bears. Pages 25–37 *in* M. Taylor, editor. Density-dependent population regulation of black, brown, and polar bears. Monograph 3. Ninth International Conference on Bear Research and Management, Missoula, Montana, USA.

Derocher, A. E., O. Wiig, and M. Andersen. 2002. Diet composition of polar bears in Svalbard and the western Barents Sea. Polar Biology 25:448–452.

DeWeaver, E. 2007. Uncertainty in climate model projections of Arctic sea ice decline: an evaluation relevant to polar bears. Administrative Report. U.S. Geological Survey, Alaska Science Center, Anchorage, Alaska, USA.

Dunton, K. H., J. L. Goodall, S. V. Schonberg, J. M. Grebmeier, and D. R. Maidment. 2005. Multi-decadal synthesis of benthic–pelagic coupling in the western arctic: role of cross-shelf advective processes. Deep-Sea Research II 52:3462–3477.

Durner, G. M., and S. C. Amstrup. 1996. Mass and body-dimension relationships of polar bears in northern Alaska. Wildlife Society Bulletin 24:480–484.

Durner, G. M., S. C. Amstrup, R. Nielson, and T. McDonald. 2004. Using discrete choice modeling to generate resource selection functions for female polar bears in the Beaufort Sea. Pages 107–120 *in* S. Huzurbazar, editor. Resource selection methods and applications. Proceedings of The First International Conference On Resource Selection, 13–15 January 2003, Laramie, Wyoming, USA.

Durner, G. M., D. C. Douglas, R. M. Nielson, and S. C. Amstrup. 2006. Model for autumn pelagic distribution of adult female polar bears in the Chukchi Seas, 1987–1994. Final report to U.S. Fish and Wildlife Service. U.S. Geological Survey, Alaska Science Center, Anchorage, Alaska, USA.

Fancy, S. G., L. F. Pank, D. C. Douglas, C. H. Curby, G. W. Garner, S. C. Amstrup, and W. L. Regelin. 1988. Satellite telemetry: a new tool for wildlife research and management. Resource Publication 172. U.S. Fish and Wildlife Service, Washington, D.C., USA.

Ferguson, S. H., M. K. Taylor, E. W. Born, A. Rosing-Asvid, and F. Messier. 2001. Activity and movement patterns of polar bears inhabiting consolidated versus active pack ice. Arctic 54:49–54.

Ferguson, S. H., M. K. Taylor, and F. Messier. 1997. Space use by polar bears in and around Auyuittuq National Park, Northwest Territories, during the ice-free period. Canadian Journal of Zoology 75:1585–1594.

Ferguson, S. H., M. K. Taylor, and F. Messier. 2000. Influence of sea ice dynamics on habitat selection by polar bears. Ecology 81:761–772.

Fischbach, A. S., S. C. Amstrup, and D. C. Douglas. 2007. Landward and eastward shift of Alaskan polar bear denning associated with recent sea ice changes. Polar Biology. [doi: 10.1007/s00300-007-0300-4]

Garner, G. W., S. T. Knick, and D. C. Douglas. 1990. Seasonal movements of adult female polar bears in the Bering and Chukchi Seas. International Conference on Bear Research and Management 8:216–226.

Gjertz, I., K. M. Kovacs, C. Lydersen, and Ø. Wiig. 2000. Movements and diving of bearded seal (*Erignathus barbatus*) mothers and pups during lactation and post-weaning. Polar Biology 23:559–566.

Groom, M. J., and C. H. Vynne. 2006. Habitat degradation and loss. Pages 173–212 *in* M. J. Groom, G. M. Meffe, and C. R. Caroll, editors. Principles of conservation biology. Sinauer, Sunderland, Massachusetts, USA.

Hansen, J., M. Sato, R. Ruedy, K. Lo, D. W. Lea, and M. Medina-Elizade. 2006. Global temperature change. Proceedings of the National Academy of Sciences (USA) 103:14288–14293.

Harwood, L. A., and I. Stirling. 1992. Distribution of ringed seals in the southeastern Beaufort Sea during late summer. Canadian Journal of Zoology 70:891–900.

Holland, M. M., C. M. Bitz, and B. Tremblay. 2006. Future reductions in the summer Arctic sea ice. Geophysical Research Letters 33:L23503.

IPCC. 2007. Climate change 2007: the physical science basis. Contribution of Working Group I to the Fourth Assessment Report of the Intergovernmental Panel on Climate Change. Cambridge University Press, Cambridge, UK.

Jakobsson, M., N. Z. Cherkis, J. Woodward, R. Macnab, and B. Coakley. 2000. New grid of Arctic bathymetry aids scientists and mapmakers. Eos 81:89.

Johnson, C. J., S. E. Nielson, E. H. Merrill, T. L. McDonald, and M. S. Boyce. 2006. Resource selection functions based on use-availability data: theoretical motivation and evaluation methods. Journal of Wildlife Management 70:347–357.

Kaufman, D.S. et al. 2004. Holocene thermal maximum in the western Arctic (0–180° W). Quaternary Science Reviews 23: 529–560.

Keating, K. A., W. G. Brewster, and C. H. Key. 1991. Satellite telemetry: performance of animal-tracking systems. Journal of Wildlife Management 55:160–171.

Kochnev, A. A. 2006. Research on polar bear autumn aggregations on Chukotka, 1989–2004. Pages 157–165 *in* J. Aars, N. J. Lunn, and A. E. Derocher, editors. Polar bears. Proceedings of the 14th Working Meeting of the IUCN/SSC Polar Bear Specialist Group, 20–24 June 2005, Seattle, Washington, USA.

Kuhfeld, W. F. 2000. Multinomial logit, discrete choice modeling: an introduction to designing choice experiments, and collecting, processing, and analyzing choice data with the SAS System. Technical Report TS-621. SAS Institute, Cary, North Carolina, USA.

Kurten, B. 1964. Evolution of the polar bear *Ursus maritimus* Phipps. Acta Zoologica Fennica 108:1–30.

Kwok, R., G. F. Cunningham, and S. S. Pang. 2004. Fram Strait sea ice outflow. Journal of Geophysical Research 109: C01009.

Lunn, N. J., I. Stirling, and D. Andriashek. 1995. Movements and distribution of polar bears in the northeastern Beaufort Sea and Western M'Clure Strait. Final report to the Inuvialuit Wildlife Management Advisory Committee. Canadian Wildlife Service, Edmonton, Alberta, Canada.

Macdonald, R. W., and J. M. Bewers. 1996. Contaminants in the Arctic marine environment: priorities for protection. ICES Journal of Marine Sciences 53:537–563.

Manly, B. F. J., L. L. McDonald, D. L. Thomas, T. L. McDonald, and W. P. Erickson. 2002. Resource selection by animals statistical design and analysis for field studies. Second edition. Kluwer Academic Publishers, Dordrecht, The Netherlands.

Maslanik, J. A., S. Drobot, C. Fowler, W. Emery, and R. Barry. 2007*a*. On the Arctic climate paradox and the continuing role of atmospheric circulation in affecting sea ice conditions. Geophysical Research Letters 34:L03711.

Maslanik, J. A., C. Fowler, J. Stroeve, S. Drobot, J. Zwally, D. Yi, and W. Emery. 2007*b*. A younger, thinner Arctic ice cover: increased potential for rapid, extensive sea ice loss. Geophysical Research Letters 34:L24501. [doi: 10.1029/2007GL032043]

Mauritzen, M., S. E. Belikov, A. N. Boltunov, A. E. Derocher, E. Hanson, R. A. Ims, Ø. Wiig, and N. Yoccoz. 2003*a*. Functional responses in polar bear habitat selection. Oikos 100:112–124.

Mauritzen, M., A. E. Derocher, O. Pavlova, and Ø. Wiig. 2003*b*. Female polar bears, *Ursus maritimus*, on the Barents Sea drift ice: walking the treadmill. Animal Behaviour 66: 107–113.

Mauritzen, M., A. E. Derocher, and Ø. Wiig. 2001. Space-use strategies of female polar bears in a dynamic sea ice habitat. Canadian Journal of Zoology 79:1704–1713.

Mauritzen, M., A. E. Derocher, Ø. Wiig, S. E. Belikov, A. N. Boltunov, E. Hansen, and G. W. Garner. 2002. Using satellite telemetry to define spatial population structure in polar bears in the Norwegian and western Russian Arctic. Journal of Applied Ecology 39:79–90.

McCracken, M. L., B. J. F. Manly, and M. Vander Heyden. 1998. Use of discrete-choice models for evaluating resource selection. Journal of Agricultural, Biological, and Environmental Statistics 3:268–279.

McLoughlin, P. D., M. S. Boyce, T. Coulson, and T. Clutton-Brock. 2006. Lifetime reproductive success and density-dependent, multi-variable resource selection. Proceedings of the Royal Society B 273:1449–1454.

Meehl, G., C. Covey, B. McAvaney, M. Latif, and R. Stouffer. 2005. Overview of the coupled model intercomparison project. Bulletin of the American Meteorological Society 86:89–93.

Meier, W., F. Fetterer, K. Knowles, M. Savoie, and M. J. Brodzik. 2006. Sea ice concentrations from Nimbus-7 SMMR and DMSP SSM/I passive microwave data, monthly averages for July 2006–December 2006. National Snow and Ice Data Center, Boulder, Colorado, USA.

Meier, W. N., J. Stroeve, and F. Fetterer. 2007. Whither Arctic sea ice? A clear signal of decline regionally, seasonally and extending beyond the satellite record. Annals of Glaciology 46:428–434.

Monnett, C., and J. S. Gleason. 2006. Observations of mortality associated with extended open-water swimming by polar bears in the Alaskan Beaufort Sea. Polar Biology 29:681–687.

Nakicencovic, N., and R. Swart. 2000. Special report on emissions scenarios. Cambridge University Press, Cambridge, UK.

Ogi, M., and J. M. Wallace. 2007. Summer minimum Arctic sea ice extent and the associated summer atmospheric circulation. Geophysical Research Letters 34:L12705.

Overland, J. E., and M. Wang. 2007. Future regional Arctic Sea ice declines. Geophysical Research Letters 34:L17005.

Pomeroy, L. R. 1997. Primary production in the Arctic Ocean estimated from dissolved oxygen. Journal of Marine Systems 10:1–8.

Ramsay, M. A., and K. A. Hobson. 1991. Polar bears make little use of terrestrial food webs: evidence from stable-carbon isotope analysis. Oecologica 86:598–600.

Ramsay, M. A., and I. Stirling. 1990. Fidelity of female polar bears to winter-den sites. Journal of Mammalogy 71:233–236.

Rayner, N. A., D. E. Parker, E. B. Horton, C. K. Folland, V. L. V. Alexander, and D. P. Rowell. 2003. Global analyses of sea surface temperature, sea ice, and night marine air temperature since the late nineteenth century. Journal of Geophysical Research 108(D14):4407.

Regehr, E. V., N. J. Lunn, S. C. Amstrup, and I. Stirling. 2007. Effects of earlier sea ice breakup on survival and population size of polar bears in western Hudson Bay. Journal of Wildlife Management 71:2673–2683.

Rigor, I. G., and J. M. Wallace. 2004. Variations in the age of Arctic sea ice and summer sea ice extent. Geophysical Research Letters 31:L09401.

Rigor, I. G., J. M. Wallace, and R. L. Colony. 2002. Response of sea ice to the Arctic Oscillation. Journal of Climate 15: 2648–2663.

Rothrock, D. A., Y. Yu, and G. A. Maykut. 1999. Thinning of the Arctic sea ice cover. Geophysical Research Letters 26: 3469–3472.

Sakshaug, E. 2003. Primary and secondary production in the Arctic seas. Page 57–81 *in* R. Stein and R. W. MacDonald, editors. The organic carbon cycle in the Arctic Ocean. Springer-Verlag, Berlin, Germany.

SAS Institute. 2000. SAS/STAT Users Guide. SAS Institute, Cary, North Carolina, USA.

Serreze, M. C., M. M. Holland, and J. Stroeve. 2007. Perspectives on the Arctic's shrinking sea ice cover. Science 315:1533–1536.

Smith, T. G. 1980. Polar bear predation of ringed and bearded seals in the land-fast sea ice habitat. Canadian Journal of Zoology 58:2201–2209.

Smith, T. G., and I. Stirling. 1975. The breeding habitat of the ringed seal (*Phoca hispida*). The birth lair and associated structures. Canadian Journal of Zoology 53:1297–1305.

Stirling, I. 1980. The biological importance of polynyas in the Canadian Arctic. Arctic 33:303–315.

Stirling, I. 1997. Importance of polynyas, ice edges, and leads to marine mammals and birds. Journal of Marine Systems 10: 9–21.

Stirling, I., D. Andriashek, and W. Calvert. 1993. Habitat preferences of polar bears in the western Canadian Arctic in late winter and spring. Polar Record 29:13–24.

Stirling, I., and W. R. Archibald. 1977. Aspects of predation of seals by polar bears. Journal of the Fisheries Research Board of Canada 34:1126–1129.

Stirling, I., N. J. Lunn, and J. Iacozza. 1999. Long-term trends in the population ecology of polar bears in western Hudson Bay in relation to climate change. Arctic 52:294–306.

Stirling, I., and N. A. Øritsland. 1995. Relationships between estimates of ringed seal (*Phoca hispida*) and polar bear (*Ursus maritimus*) populations in the Canadian Arctic. Canadian Journal of Fisheries and Aquatic Science 52:2594–2612.

Stirling, I., and C. L. Parkinson. 2006. Possible effects of a warming climate on selected populations of polar bears (*Ursus maritimus*) in the Canadian Arctic. Arctic 59:261–275.

Stirling, I., C. Spencer, and D. Andriashek. 1989. Immobilization of polar bears (*Ursus maritimus*) with Telazol. Journal of Wildlife Diseases 25:159–168.

Stroeve, J., M. M. Holland, W. Meier, T. Scambos, and M. Serreze. 2007. Arctic sea ice decline: faster than forecast. Geophysical Research Letters 34:L09501.

Stroeve, J., M. C. Serreze, F. Fetterer, T. Arbetter, W. Meier, J. Maslanik, and K. Knowles. 2005. Tracking the Arctic's shrinking ice cover: another extreme September minimum in 2004. Geophysical Research Letters 32:L04501.

Taylor, M. K., S. Akeeagok, D. Andriashek, W. Barbour, E. W. Born, W. Calvert, H. D. Cluff, S. Ferguson, J. Laake, A. Rosing-Asvid, I. Stirling, and F. Messier. 2001. Delineating Canadian and Greenland polar bear (*Ursus maritimus*) populations by cluster analysis. Canadian Journal of Zoology 79:690–709.

Thiemann, G. W., S. J. Iverson, and I. Stirling. 2005. Seasonal, sexual and anatomical variability in the adipose tissue of polar bears (*Ursus maritimus*). Journal of Zoology 269:65–76.

Tucker, W. B., J. W. Weatherly, D. T. Eppler, L. D. Farmer, and D. L. Bentley. 2001. Evidence for rapid thinning of sea ice in the western Arctic Ocean at the end of the 1980s. Geophysical Research Letters 28:2851–2854.

USFWS (U.S. Fish and Wildlife Service). 2007. Endangered and threatened wildlife and plants; 12-month petition finding and proposed rule to list the polar bear (*Ursus maritimus*) as Threatened throughout its range. Federal Register 72(5):9 January 2007.

Viranta, S. 2003. Geographic and temporal ranges of middle and late Miocene carnivores. Journal of Mammalogy 84: 1267–1278.

Wadhams, P. 2000. Ice in the ocean. Gordon and Breach Science Publishers, Amsterdam, The Netherlands.

Wilcove, D. S., D. Rothstein, J. Dubow, A. Phillips, and E. Losos. 1998. Quantifying threats to imperiled species in the United States. BioScience 48:607–615.

Woodgate, R. A., K. Aagaard, and T. J. Weingartner. 2006. Interannual changes in the Bering Strait fluxes of volume, heat and freshwater between 1991 and 2004. Geophysical Research Letters 33:L15609.

Zhang, X., and J. E. Walsh. 2006. Toward a seasonally ice-covered Arctic Ocean: scenarios from the IPCC AR4 model simulations. Journal of Climate 19:1730–1747.